

A variable kinematic doubly-curved MITC9 shell element for the analysis of laminated composites

Original

A variable kinematic doubly-curved MITC9 shell element for the analysis of laminated composites / Cinefra, Maria; Valvano, Stefano. - In: MECHANICS OF ADVANCED MATERIALS AND STRUCTURES. - ISSN 1537-6494. - 23:11(2016), pp. 1312-1325. [10.1080/15376494.2015.1070304]

Availability:

This version is available at: 11583/2525505 since: 2016-05-23T16:33:48Z

Publisher:

Taylor & Francis

Published

DOI:10.1080/15376494.2015.1070304

Terms of use:

openAccess

This article is made available under terms and conditions as specified in the corresponding bibliographic description in the repository

Publisher copyright

(Article begins on next page)

A variable kinematic doubly-curved MITC9 shell element for the analysis of laminated composites

M. Cinefra¹, S. Valvano¹

(1) Department of Aeronautics and Space Engineering,
Politecnico di Torino, Turin, Italy

Keywords:

doubly-curved shells, Finite Element Method, Mixed Interpolated Tensorial Components, Carrera's Unified Formulation, laminated composites, benchmark solutions.

Author and address for Correspondence

Dr. Maria Cinefra
Research Assistant,
Department of Aeronautics and Space Engineering
Politecnico di Torino,
Corso Duca degli Abruzzi, 24,
10129 Torino, ITALY,
tel +39.011.546.6869, fax +39.011.564.6899
e.mail: maria.cinefra@polito.it

Abstract

The present paper considers the linear static analysis of composite shell structures with double-curvature geometry by means of a shell finite element with variable through-the-thickness kinematic. The refined models used are grouped in the Unified Formulation by Carrera (CUF) and they permit the distribution of displacements and stresses along the thickness of the multilayered shell to be accurately described. The shell element has nine nodes and the Mixed Interpolation of Tensorial Components (MITC) method is used to contrast the membrane and shear locking phenomenon. The governing equations are derived from the Principle of Virtual Displacement (PVD) and the Finite Element Method (FEM) is employed to solve them. Cross-ply spherical shells with simply-supported edges and subjected to bi-sinusoidal pressure are analyzed. Various laminations, thickness ratios and curvature ratios are considered. The results, obtained with different theories contained in the CUF, are compared with both the elasticity solutions given in literature and the analytical solutions obtained using the CUF and the Navier's method. From the analysis, one can conclude that the shell element based on the CUF is very efficient and its use is mandatory with respect to the classical models in the study of composite structures. Finally, shells with different lamination, boundary conditions and loads are also analyzed using high-order layer-wise theories in order to provide FEM benchmark solutions.

1 Introduction

Shell structures have a predominant role in a variety of engineering applications thanks to their efficient load-carrying capabilities. On the other hand, the continuous development of new structural materials, such as composite layered materials, leads to increasingly complex structural designs that require careful analysis.

Anisotropy, nonlinear analysis as well as complicating effects, such as the C_z^0 - Requirements (zig-zag effects in the displacements and interlaminar continuity for the stresses), the couplings between in-plane and out-of-plane strains, make the analysis of layered composite structures complicated in practice. Analytical, closed form solutions are available in very few cases. In most of the practical problems, the solution demand applications of approximated computational methods.

Many computational techniques have been developed and applied to layered constructions. A full mixed 3D finite difference technique was developed by Noor and Rarig [1]. More recently, a differential quadrature technique has been proposed by Malik [2], Malik and Bert [3] and applied by Liew et al. [4]. A boundary element formulation has been employed by Dav in [5]. In [6]-[8], Ferreira et al. adopt a meshless collocation method based on the use of Radial Basis Functions (RBF) for the analysis of laminated plates and shells. Exhaustive overviews on several computational techniques and their applications to laminated structures can be read in the review articles [9]-[11].

Among the computational techniques implemented for the analysis of layered structures, a predominant role has been played by Finite Element Method (FEM). The most of finite elements available in literature are formulated on the bases of axiomatic-type theories, in which the unknown variables are postulated along the thickness. According to MacNeal [12] the first FEM analysis was published in 1961. The majority of early FEM calculations were performed with the classical Kirchhoff-Love theory and some examples are given in [13]-[17]. But, it was difficult to satisfy the requirements of compatibility in thin shell analysis because the rotations were derived from the transversal displacement. For this reason, plate/shell elements based on the First-order Shear Deformation Theory (FSDT) were developed by Pryor and Barker [18], Noor [19], Hughes [20], Panda and Natarayan [21], Parisch [22], Ferreira [23] and many others. However, early FSDT type elements showed severe stiffening in thin plate/shell limits. Such a numerical mechanism, known as shear or membrane locking, was first contrasted by implementation of numerical tricks, such as reduced/selective integration schemes [24]-[28].

But, spurious zero energy modes are introduced by these sub-integration techniques. In [29] and [30], Chinosi et al. developed a hierarchic finite element for thin Naghdi shell model [31] that was able to contrast locking for the shell problem in its displacement formulation. However, in the case of very small thickness and when the element is not of degree as high as needed, the numerical solution exhibits a loss in the rate of convergence due to the locking. The so-called Mixed Interpolation of Tensorial Components (MITC) was implemented to overcome both these problems. Many articles by Bathe and others are available on that topic: examples are the papers [32]-[37]. Arnold and Brezzi [38] dealt with a mixed formulation of the Nagdi model, giving a family of locking free elements and proving the convergence of their numerical approach. Similarly, Ramm and Bischoff [39]-[43] developed a shell finite element based on a 7-parameter theory, in which the extra strain term is incorporated via the enhanced assumed strain concept proposed by Simo and Rafai [44].

Also a large variety of plate/shell finite element implementations of higher-order theories (HOT) have been proposed in the last twenty years literature. HOT-based C^0 finite elements (C^0 means that the continuity is required only for the unknown variables and not for their derivatives) were discussed by Kant and co-authors [45],[46]. In [47]-[51], Polit et al. proposed a C^1 six-nodes triangular finite element in which the transverse shear strains are represented by cosine functions. This element is able to ensure both the continuity conditions for displacements and transverse shear stresses at the interfaces between layers of laminated structures. A comprehensive discussion of HOT-type theories and related finite element suitability has been provided by Tessler [52]. Many other papers are available in which HOTs have been implemented for plates and shells, details can be found in the books by Reddy [53] and Palazotto and Dennis [54].

Dozens of finite elements have been proposed based on zig-zag theories [55],[56]. An application of Reissner Mixed Variational Theorem (RMVT) [57] to develop standard finite elements was proposed by Rao and Meyer-Piening [58]. A generalization of RMVT as a tool to develop approximate solutions was given by Carrera [59]. The obtained finite elements represent the FE implementation of the Murakami theory [60] and were denoted by the acronym RMZC, (Reissner Mindlin Zigzag interlaminar Continuity). Full extensions of RMZC to shell geometries have been done by Brank and Carrera [61]. Finally, finite element implementations of layer-wise theories in the framework of axiomatic-type theories have been proposed by many authors, among which Noor and Burton [62], Reddy [63], Mawenya and Davies [64], Pinsky and Kim [65], Chaudhuri and Seide [66], Rammerstorfer et al. [67].

An improved doubly-curved shell finite element is here presented for the analysis of composite structures. It is based on the Carrera's Unified Formulation (CUF), which was developed by Carrera for multi-layered structures [68],[69]. Both Equivalent Single Layer (ESL) and Layer Wise (LW) theories contained in the CUF have been implemented in the shell finite element. The Mixed Interpolation of Tensorial Components (MITC) method [70]-[73] is used to contrast the membrane and shear locking. The governing equations for the linear static analysis of composite structures are derived from the Principle of Virtual Displacement (PVD), in order to apply the finite element method. Cross-ply spherical shells with simply-supported edges and subjected to bi-sinusoidal load are analyzed. The results, obtained with the different models contained in the CUF, are compared with the exact solution given in literature. Also FEM benchmark solutions regarding doubly-curved shells with different laminations, boundary conditions and loads are provided.

2 Unified Formulation

The main feature of the Unified Formulation by Carrera [59] (CUF) is the unified manner in which the displacement variables are handled. In the framework of the CUF, the displacement field is written by means of approximating functions in the thickness direction as follows:

$$\delta \mathbf{u}^k(\alpha, \beta, z) = F_\tau(z) \delta \mathbf{u}_\tau^k(\alpha, \beta); \quad \mathbf{u}^k(\alpha, \beta, z) = F_s(z) \mathbf{u}_s^k(\alpha, \beta) \quad \tau, s = 0, 1, \dots, N \quad (1)$$

where (α, β, z) is a curvilinear reference system, in which α and β are orthogonal and the curvature radii R_α and R_β are constant in each point of the domain Ω (see Fig. 1). The displacement vector $\mathbf{u} = \{u, v, w\}$ has its components expressed in this system. $\delta\mathbf{u}$ indicates the virtual displacement associated to the virtual work and k identifies the layer. F_τ and F_s are the so-called thickness functions depending only on z . \mathbf{u}_s are the unknown variables depending on the coordinates α and β . τ and s are sum indexes and N is the order of expansion in the thickness direction assumed for the displacements.

In the case of Equivalent Single Layer (ESL) models, a Taylor expansion is employed as thickness functions:

$$\mathbf{u} = F_0 \mathbf{u}_0 + F_1 \mathbf{u}_1 + \dots + F_N \mathbf{u}_N = F_s \mathbf{u}_s, \quad s = 0, 1, \dots, N. \quad (2)$$

$$F_0 = z^0 = 1, \quad F_1 = z^1 = z, \quad \dots, \quad F_N = z^N. \quad (3)$$

Classical models, such as those based on the First-order Shear Deformation Theory (FSDT) [31], can be obtained from an ESL theory with $N = 1$, by imposing a constant transverse displacement through the thickness via penalty techniques. Also a model based on the hypotheses of Classical Lamination Theory (CLT) [74],[75] can be expressed by means of the CUF by applying a penalty technique to the constitutive equations (see section 4). This permits to impose that the transverse shear strains are null in the shell.

In the case of Layer-Wise (LW) models, the displacement is defined at k -layer level:

$$\mathbf{u}^k = F_t \mathbf{u}_t^k + F_b \mathbf{u}_b^k + F_r \mathbf{u}_r^k = F_s \mathbf{u}_s^k, \quad s = t, b, r, \quad r = 2, \dots, N. \quad (4)$$

$$F_t = \frac{P_0 + P_1}{2}, \quad F_b = \frac{P_0 - P_1}{2}, \quad F_r = P_r - P_{r-2}. \quad (5)$$

in which $P_j = P_j(\zeta_k)$ is the Legendre polynomial of j -order defined in the ζ_k -domain: $-1 \leq \zeta_k \leq 1$. The top (t) and bottom (b) values of the displacements are used as unknown variables and one can impose the following compatibility conditions:

$$u_t^k = u_b^{k+1}, \quad k = 1, N_l - 1. \quad (6)$$

The LW models, in respect to the ESLs, allow the zig-zag form of the displacement distribution in layered structures to be modelled. It is possible to reproduce the zig-zag effects also in the framework of the ESL description by employing the Murakami theory. According to references [60], a zig-zag term can be introduced into equation (2) as follows:

$$\mathbf{u}^k = F_0 \mathbf{u}_0^k + \dots + F_N \mathbf{u}_N^k + (-1)^k \zeta_k \mathbf{u}_Z^k. \quad (7)$$

Subscript Z refers to the introduced term. Such theories are called zig-zag (ZZ) theories.

3 MITC9 shell element

In this section, the derivation of a shell finite element for the analysis of multilayered structures is presented. The element is based on both the ESL, ZZ and LW theories contained in the Unified Formulation. A nine-nodes element with doubly-curved geometry is considered. After an overview in scientific literature about the methods that permit to withstand the membrane and shear locking, the MITC technique has been adopted for this element.

3.1 Geometrical relations

Shells are bi-dimensional structures in which one dimension (in general the thickness in z direction) is negligible with respect to the other two in-plane dimensions. Geometry and the reference system are indicated in Fig. 1. By considering multilayered structures, the square of an infinitesimal linear segment in the layer, the associated infinitesimal area and volume are given by:

$$\begin{aligned} ds_k^2 &= H_\alpha^{k2} d\alpha_k^2 + H_\beta^{k2} d\beta_k^2 + H_z^{k2} dz_k^2, \\ d\Omega_k &= H_\alpha^k H_\beta^k d\alpha_k d\beta_k, \\ dV &= H_\alpha^k H_\beta^k H_z^k d\alpha_k d\beta_k dz_k, \end{aligned} \quad (8)$$

where the metric coefficients are:

$$H_\alpha^k = A^k(1 + z_k/R_\alpha^k), \quad H_\beta^k = B^k(1 + z_k/R_\beta^k), \quad H_z^k = 1. \quad (9)$$

k denotes the k -layer of the multilayered shell; R_α^k and R_β^k are the principal radii of the midsurface of the layer k . A^k and B^k are the coefficients of the first fundamental form of Ω_k (Γ_k is the Ω_k boundary). In this paper, the attention has been restricted to shells with constant radii of curvature (cylindrical, spherical, toroidal geometries) for which $A^k = B^k = 1$. Details for shells are reported in [76].

Geometrical relations permit the in-plane ϵ_p^k and out-plane ϵ_n^k strains to be expressed in terms of the displacement \mathbf{u} . The following relations hold:

$$\epsilon_p^k = [\epsilon_{\alpha\alpha}^k, \epsilon_{\beta\beta}^k, \epsilon_{\alpha\beta}^k]^T = (\mathbf{D}_p^k + \mathbf{A}_p^k) \mathbf{u}^k, \quad \epsilon_n^k = [\epsilon_{\alpha z}^k, \epsilon_{\beta z}^k, \epsilon_{zz}^k]^T = (\mathbf{D}_{n\Omega}^k + \mathbf{D}_{nz}^k - \mathbf{A}_n^k) \mathbf{u}^k. \quad (10)$$

The explicit form of the introduced arrays is:

$$\mathbf{D}_p^k = \begin{bmatrix} \frac{\partial_\alpha}{H_\alpha^k} & 0 & 0 \\ 0 & \frac{\partial_\beta}{H_\beta^k} & 0 \\ \frac{\partial_\beta}{H_\beta^k} & \frac{\partial_\alpha}{H_\alpha^k} & 0 \end{bmatrix}, \quad \mathbf{D}_{n\Omega}^k = \begin{bmatrix} 0 & 0 & \frac{\partial_\alpha}{H_\alpha^k} \\ 0 & 0 & \frac{\partial_\beta}{H_\beta^k} \\ 0 & 0 & 0 \end{bmatrix}, \quad \mathbf{D}_{nz}^k = \begin{bmatrix} \partial_z & 0 & 0 \\ 0 & \partial_z & 0 \\ 0 & 0 & \partial_z \end{bmatrix}, \quad (11)$$

$$\mathbf{A}_p^k = \begin{bmatrix} 0 & 0 & \frac{1}{H_\alpha^k R_\alpha^k} \\ 0 & 0 & \frac{1}{H_\beta^k R_\beta^k} \\ 0 & 0 & 0 \end{bmatrix}, \quad \mathbf{A}_n^k = \begin{bmatrix} \frac{1}{H_\alpha^k R_\alpha^k} & 0 & 0 \\ 0 & \frac{1}{H_\beta^k R_\beta^k} & 0 \\ 0 & 0 & 0 \end{bmatrix}. \quad (12)$$

3.2 MITC method

Considering a 9-nodes finite element, the displacement components are interpolated on the nodes of the element by means of the Lagrangian shape functions N_i :

$$\delta \mathbf{u}_\tau = N_i \delta \mathbf{u}_{\tau_i} \quad \mathbf{u}_s = N_j \mathbf{u}_{s_j} \quad \text{with } i, j = 1, \dots, 9 \quad (13)$$

where \mathbf{u}_{s_j} and $\delta \mathbf{u}_{\tau_i}$ are the nodal displacements and their virtual variations. Substituting in the geometrical relations (10) one has:

$$\begin{aligned} \epsilon_p &= F_\tau(\mathbf{D}_p + \mathbf{A}_p)(N_i \mathbf{I}) \mathbf{u}_{\tau_i} \\ \epsilon_n &= F_\tau(\mathbf{D}_{n\Omega} - \mathbf{A}_n)(N_i \mathbf{I}) \mathbf{u}_{\tau_i} + F_{\tau,z}(N_i \mathbf{I}) \mathbf{u}_{\tau_i} \end{aligned} \quad (14)$$

where \mathbf{I} is the identity matrix.

Considering the local coordinate system (ξ, η) , the MITC shell elements ([77]-[79]) are formulated by using, instead of the strain components directly computed from the displacements, an interpolation of these within each element using a specific interpolation strategy for each component. The corresponding interpolation points, called *tying points*, are shown in Fig. 2 for a nine-nodes element. Note that the transverse normal strain ϵ_{zz} is excluded from this procedure and it is directly calculated from the displacements.

The interpolating functions are Lagrangian functions and are arranged in the following arrays:

$$\begin{aligned} N_{m1} &= [N_{A1}, N_{B1}, N_{C1}, N_{D1}, N_{E1}, N_{F1}] \\ N_{m2} &= [N_{A2}, N_{B2}, N_{C2}, N_{D2}, N_{E2}, N_{F2}] \\ N_{m3} &= [N_P, N_Q, N_R, N_S] \end{aligned} \quad (15)$$

From this point on, the subscripts $m1$, $m2$ and $m3$ indicate quantities calculated in the points $(A1, B1, C1, D1, E1, F1)$, $(A2, B2, C2, D2, E2, F2)$ and (P, Q, R, S) , respectively. Therefore, the strain components are interpolated as follows:

$$\begin{aligned} \epsilon_p &= \begin{bmatrix} \epsilon_{\alpha\alpha} \\ \epsilon_{\beta\beta} \\ \epsilon_{\alpha\beta} \end{bmatrix} = \begin{bmatrix} N_{m1} & 0 & 0 \\ 0 & N_{m2} & 0 \\ 0 & 0 & N_{m3} \end{bmatrix} \begin{bmatrix} \epsilon_{\alpha\alpha_{m1}} \\ \epsilon_{\beta\beta_{m2}} \\ \epsilon_{\alpha\beta_{m3}} \end{bmatrix} \\ \epsilon_n &= \begin{bmatrix} \epsilon_{\alpha z} \\ \epsilon_{\beta z} \\ \epsilon_{zz} \end{bmatrix} = \begin{bmatrix} N_{m1} & 0 & 0 \\ 0 & N_{m2} & 0 \\ 0 & 0 & 1 \end{bmatrix} \begin{bmatrix} \epsilon_{\alpha z_{m1}} \\ \epsilon_{\beta z_{m2}} \\ \epsilon_{zz} \end{bmatrix} \end{aligned} \quad (16)$$

where the strains $\epsilon_{\alpha\alpha_{m1}}$, $\epsilon_{\beta\beta_{m2}}$, $\epsilon_{\alpha\beta_{m3}}$, $\epsilon_{\alpha z_{m1}}$, $\epsilon_{\beta z_{m2}}$ are expressed by means of eq.s (14) in which the shape functions N_i and their derivatives are evaluated in the tying points. For example, one can considers the strain component $\epsilon_{\alpha\alpha}$ that is calculated as follows:

$$\epsilon_{\alpha\alpha} = N_{A1}\epsilon_{\alpha\alpha_{A1}} + N_{B1}\epsilon_{\alpha\alpha_{B1}} + N_{C1}\epsilon_{\alpha\alpha_{C1}} + N_{D1}\epsilon_{\alpha\alpha_{D1}} + N_{E1}\epsilon_{\alpha\alpha_{E1}} + N_{F1}\epsilon_{\alpha\alpha_{F1}} \quad (17)$$

with:

$$\epsilon_{\alpha\alpha_{A1}} = N_{i,\alpha}^{(A1)} F_\tau u_{\tau_i} + \frac{1}{H_\alpha R_\alpha} N_i^{(A1)} F_\tau w_{\tau_i} \quad (18)$$

The superscript $(A1)$ indicates that the shape function and its derivative are evaluated in the point of coordinates $(-\frac{1}{\sqrt{3}}, -\sqrt{\frac{3}{5}})$. Similar expressions can be written for $\epsilon_{\alpha\alpha_{B1}}, \epsilon_{\alpha\alpha_{C1}}, \epsilon_{\alpha\alpha_{D1}}, \epsilon_{\alpha\alpha_{E1}}, \epsilon_{\alpha\alpha_{F1}}$.

4 Constitutive equations

The second step towards the governing equations is the definition of the 3D constitutive equations that permit to express the stresses by means of the strains. The generalized Hooke's law is considered, by employing a linear constitutive model for infinitesimal deformations. In a composite material, these

equations are obtained in material coordinates $(1, 2, 3)$ for each orthotropic layer k and then rotated in the general curvilinear reference system (α, β, z) .

Therefore, the stress-strain relations after the rotation are:

$$\begin{aligned}\boldsymbol{\sigma}_p^k &= \mathbf{C}_{pp}^k \boldsymbol{\epsilon}_p^k + \mathbf{C}_{pn}^k \boldsymbol{\epsilon}_n^k \\ \boldsymbol{\sigma}_n^k &= \mathbf{C}_{np}^k \boldsymbol{\epsilon}_p^k + \mathbf{C}_{nn}^k \boldsymbol{\epsilon}_n^k\end{aligned}\tag{19}$$

where

$$\begin{aligned}\mathbf{C}_{pp}^k &= \begin{bmatrix} C_{11}^k & C_{12}^k & C_{16}^k \\ C_{12}^k & C_{22}^k & C_{26}^k \\ C_{16}^k & C_{26}^k & C_{66}^k \end{bmatrix} & \mathbf{C}_{pn}^k &= \begin{bmatrix} 0 & 0 & C_{13}^k \\ 0 & 0 & C_{23}^k \\ 0 & 0 & C_{36}^k \end{bmatrix} \\ \mathbf{C}_{np}^k &= \begin{bmatrix} 0 & 0 & 0 \\ 0 & 0 & 0 \\ C_{13}^k & C_{23}^k & C_{36}^k \end{bmatrix} & \mathbf{C}_{nn}^k &= \begin{bmatrix} C_{55}^k & C_{45}^k & 0 \\ C_{45}^k & C_{44}^k & 0 \\ 0 & 0 & C_{33}^k \end{bmatrix}\end{aligned}\tag{20}$$

The material coefficients C_{ij} depend on the Young's moduli E_1, E_2, E_3 , the shear moduli G_{12}, G_{13}, G_{23} and Poisson moduli $\nu_{12}, \nu_{13}, \nu_{23}, \nu_{21}, \nu_{31}, \nu_{32}$ that characterize the layer material.

5 Governing equations

This section presents the derivation of the governing finite element stiffness matrix based on the Principle of Virtual Displacement (PVD) in the case of multi-layered doubly-curved shells subjected to mechanical loads.

The PVD for a multilayered doubly-curved shell reads:

$$\int_{\Omega_k} \int_{A_k} \left\{ \delta \boldsymbol{\epsilon}_p^{kT} \boldsymbol{\sigma}_p^k + \delta \boldsymbol{\epsilon}_n^{kT} \boldsymbol{\sigma}_n^k \right\} H_\alpha^k H_\beta^k d\Omega_k dz = \int_{\Omega_k} \int_{A_k} \delta \mathbf{u}^k \mathbf{p}^k H_\alpha^k H_\beta^k d\Omega_k dz\tag{21}$$

where Ω_k and A_k are the integration domains in the plane and in the thickness direction, respectively. The first member of the equation represents the variation of the internal work, while the second member is the external work. $\mathbf{p}^k = \mathbf{p}^k(\alpha, \beta, z)$ is the mechanical load applied to the structure at layer level.

Substituting the constitutive equations (19), the geometrical relations written via the MITC method (16) and applying the Unified Formulation (1) and the FEM approximation (13), one obtains the following governing equations:

$$\delta \mathbf{q}_{\tau_i}^k : \mathbf{K}^{k\tau sij} \mathbf{q}_{s_j}^k = \mathbf{P}_{\tau_i}^k\tag{22}$$

where $\mathbf{K}^{k\tau sij}$ is a 3×3 matrix, called fundamental nucleus, and its explicit expression is given in Appendix. This is the basic element from which the stiffness matrix of the whole structure is computed. The fundamental nucleus is expanded on the indexes τ and s in order to obtain the stiffness matrix of each layer. Then, the matrixes of each layer are assembled at multi-layer level depending on the approach considered, ESL or LW. $\mathbf{P}_{\tau_i}^k$ is the fundamental nucleus for the external mechanical load. For more details, the reader can refer to [68].

6 Acronyms

Several refined and advanced two-dimensional models are contained in the Unified Formulation. Depending on the variables description (LW, ESL or ZZ) and the order of expansion N of the displacements

in ξ_3 , a large variety of kinematics shell theories can be obtained. A system of acronyms is given in order to denote these models. The first letter indicates the multi-layer approach which can be Equivalent Single Layer (E) or Layer Wise (L). The number N indicates the order of expansion used in the thickness direction (from 1 to 4). In the case of LW approach, the same order of expansion is used for each layer. In the case of ESL approach, a letter Z can be added if the zig-zag effects of displacements is considered by means of Murakami's zig-zag function. Summarizing, E1-E4 are ESL models. If Murakami zigzag function is used, these equivalent single layer models are indicated as EZ1-EZ3. In the case of layer wise approaches, the letter L is considered in place of E, so the acronyms are L1-L4. Classical theories such as Classical Lamination Theory (CLT) and First order Shear Deformation Theory (FSDT), can be obtained as particular cases of E1 theory simply imposing constant value of w through the thickness direction. An appropriate application of penalty technique to shear moduli of the material leads to CLT.

7 Numerical results

This section is composed of two parts. The first one is devoted to the assessment of the shell element based on the Unified Formulation by the static analysis of simply supported spherical shells under bi-sinusoidal load. Using the theory that provides the most accurate results, the second part presents some benchmark solutions relative to spherical shells with particular lamination, boundary conditions and load.

7.1 Assessment

In order to assess the robustness of the present shell element and show the efficiency of CUF in the analysis of laminated composites, some numerical results for simply-supported cross-ply square shells are presented. These are compared with the 3D solutions given in [80] and the solutions of the higher-order shell theory (HSDT₁) discussed in [81]. The analytical solution L4_a is also provided as reference solution. This is obtained using the L4 theory and the Navier's method to solve the governing equations in closed form. In [82], it was demonstrated that the L4_a solutions can be considered quasi-3D. Being a the length of the edge and $R = R_\alpha = R_\beta$ the curvature radius, deep ($R/a = 1, 2$) and shallow ($R/a = 5$) shells are examined. The lamination schemes ($0^\circ, 90^\circ \dots$) are of symmetric and anti-symmetric type with number of layers $N_l = 3, 5$ and $N_l = 4$, respectively. The shell is subjected to a bi-sinusoidal pressure applied at the top surface $p_z^+ = \hat{p}_z^+ \sin(\pi\alpha/a) \sin(\pi\beta/a)$, where m, n are the numbers of half-waves. The lamina material properties and the load parameters are given in Table 1. The following nondimensionalized deflections and stresses are considered:

$$\begin{aligned} \bar{w} &= w(a/2, a/2) \frac{100 E_{22} h^3}{a^4 \hat{p}_z^+} ; & \bar{\sigma}_{\alpha\alpha} &= \sigma_{\alpha\alpha}(a/2, a/2) \frac{h^2}{a^2 \hat{p}_z^+} \\ \bar{\sigma}_{\alpha z} &= \sigma_{\alpha z}(0, a/2) \frac{h}{a \hat{p}_z^+} ; & \bar{\sigma}_{zz} &= \sigma_{zz}(a/2, a/2) \frac{1}{\hat{p}_z^+} \end{aligned} \quad (23)$$

For brevity reasons, the convergence study is here omitted, but it has been verified that a mesh (9×9) permits the convergence solution to be reached. All the results are calculated using this mesh. Tables 2-4 present results in terms of transversal displacement \bar{w} for the three lamination cases. Different thickness ratios a/h and curvature ratios R/a are considered and various theories contained in the Unified Formulation are used. One can note that, in thin shells ($a/h = 100$), all the theories, comprising CLT and FSDT, match the reference solutions (3D, HSDT₁ and L4_a). While, increasing the thickness, higher-order models are required. In particular, higher-order zig-zag models work better than ESL ones and LW better than zig-zag. The L4 theory is able to reproduce the reference solutions in all the cases

considered. There are no differences in the behavior of the element between deep and shallow shells because, in the formulation of the models, no assumptions have been made about the curvature. The same considerations can be made considering both symmetric and anti-symmetric laminations.

In the symmetric case with $N_l = 3$, the normal stress $\bar{\sigma}_{\alpha\alpha}$ is also evaluated (see Table 5). The behavior of the element is the same. Higher-order models are necessary in the analysis of thick shells. The L4 theory doesn't match perfectly the reference solutions but provides very good results. The shear stress $\bar{\sigma}_{\alpha z}$ is reported in Table 6 for the different laminations and considering $R/a = 2$. Good results are obtained also in this case using higher-order layer-wise theories, especially for thick shells. A slightly higher error can be observed only in the case of antisymmetric lamination. Figures 3-6 and 7-10 show the distributions along the thickness of the shear stress $\bar{\sigma}_{\alpha z}$ and the normal stress $\bar{\sigma}_{zz}$ for different combinations of R/a and a/h in the symmetric $N_l = 3$ and the antisymmetric $N_l = 4$ case. In all the cases, one can note that only the layer-wise model is able to fulfill the continuity conditions of the transverse stresses at the interface between layers.

7.2 FEM benchmark solutions

Similar spherical shells are analyzed, considering three new problems that have not reference analytical solutions:

1. Shell with anti-symmetric lamination ($45^\circ / -45^\circ$) under bi-sinusoidal load and simply-supported boundary conditions.
2. Shell with clamped-free boundary conditions: edges parallel to β -direction clamped and those parallel to α -direction free. The lamination is $(0^\circ, 90^\circ, 0^\circ)$ and the load is bi-sinusoidal.
3. Shell subjected to a concentrated load (intensity $P = a^2$), applied in the central point at the top surface, with $(0^\circ, 90^\circ, 0^\circ)$ lamination and simply-supported boundary conditions.

The material properties and load parameters are given in Table 1. The solutions are calculated using a (9×9) mesh and the L4 model. In order to get more accurate results, two fictitious layers are considered per each layer.

In Tables 7-9, the results are given in terms of w , $\sigma_{\alpha\alpha}$, $\sigma_{\beta\beta}$, $\sigma_{\alpha\beta}$, $\sigma_{\alpha z}$, $\sigma_{\beta z}$ and σ_{zz} for different thickness ratios a/h and curvature ratios R/a . Depending on the problem analyzed, these quantities are evaluated in different points. For problem 1, one has:

$$\begin{aligned}
w &\rightarrow (a/2, a/2, 0) \\
\sigma_{\alpha\alpha}, \sigma_{\beta\beta} &\rightarrow (a/2, a/2, \pm h/2) \\
\sigma_{\alpha\beta} &\rightarrow (0, 0, \pm h/2) \\
\sigma_{\alpha z} &\rightarrow (0, a/2, -h/12) \\
\sigma_{\beta z} &\rightarrow (a/2, 0, h/12) \\
\sigma_{zz} &\rightarrow (a/2, a/2, h/12)
\end{aligned} \tag{24}$$

for problem 2:

$$\begin{aligned}
w &\rightarrow (a/2, a/2, 0) \\
\sigma_{\alpha\alpha}, \sigma_{\beta\beta} &\rightarrow (a/2, a/2, \pm h/2) \\
\sigma_{\alpha\beta} &\rightarrow (0, 0, \pm h/2) \\
\sigma_{\alpha z} &\rightarrow (0, a/2, -h/4) \\
\sigma_{\beta z} &\rightarrow (a/2, 0, h/4) \\
\sigma_{zz} &\rightarrow (a/2, a/2, h/4)
\end{aligned} \tag{25}$$

and for problem 3:

$$\begin{aligned}
w &\rightarrow (a/2, a/2, 0) \\
\sigma_{\alpha\alpha}, \sigma_{\beta\beta} &\rightarrow (a/2, a/2, \pm h/2) \\
\sigma_{\alpha\beta} &\rightarrow (0, 0, \pm h/2) \\
\sigma_{\alpha z} &\rightarrow (0, a/2, -h/4) \\
\sigma_{\beta z} &\rightarrow (a/2, 0, h/4) \\
\sigma_{zz} &\rightarrow (a/2, a/2, h/4)
\end{aligned} \tag{26}$$

Figures 11-14 and 15-18 show the distributions along the thickness of the shear stress $\sigma_{\alpha z}$ and the normal stress σ_{zz} for different combinations of thickness ratio a/h and curvature ratio R/a for problem 1 and 2, respectively. For comparison purposes, also the EZ3 solution is represented. As in the assessment analysis, the EZ3 model is not able to satisfy the continuity conditions of transverse stresses at the interface between layers. In some cases, neither the L4 model is efficient in this sense. This fact suggests the use of mixed models based on Reissner's Mixed Variational Theorem, in which the transverse stresses are modelled a-priori (see the works [83],[84]) and future companion works can be devoted to this subject. Finally, figures 19-22 show the distributions of the shear stress $\sigma_{\alpha z}$ and the normal stress σ_{zz} by varying a/h for $R/a = 2$ and R/a for $a/h = 10$, in the case of concentrated load (problem 3).

8 Conclusions

This paper has dealt with the static analysis of composite doubly-curved shells by means of a shell finite element based on the Unified Formulation by Carrera. An assessment of the element has been performed by analyzing cross-ply spherical shells under bi-sinusoidal load and simply-supported boundary conditions. The results have been presented in terms of both transversal displacement, in plane stresses and transverse stresses, for various thickness ratios, curvature ratios and lamination schemes. The performances of the shell element have been tested and the different theories (classical and refined) contained in the CUF have been compared. The conclusions that can be drawn are the following:

1. the shell element is locking free, when the shell is very thin, and the results converge to the reference solution by increasing the order of expansion of the displacements in the thickness direction;
2. when the shell is very thick, the LW models work better than ZZ ones, and these work better than ESL models;
3. the classical models, such as CLT and FSDT fail in the analysis of thick shells;
4. the use of LW models is mandatory for both thick and thin shells, if one needs to accurately describe the distribution of transverse stresses in the thickness and to satisfy the interlaminar continuity conditions;
5. the element provides good results for both deep and shallow shells and for both symmetric and anti-symmetric lamination schemes.

Finally, some benchmark solutions have been calculated for spherical shells that have not analytical reference solutions: lamination $(45, -45)$, clamped-free boundary conditions and concentrated load have been considered. Results have been presented in terms of transversal displacement, in plane stresses and transverse stresses in the form of both tables and graphs. Future companion works could be devoted to doubly-curved shell elements based on Reissner's Mixed Variational Theorem for the a-priori modelling of the transverse stresses.

References

- [1] Noor, A.K., Rarig, P.L., “Three-Dimensional solutions of laminated cylinders,” *Computer Methods in Applied Mechanics and Engineering*, Vol. 3, 1974, pp. 319–334.
- [2] Malik, M., “Differential quadrature method in computational mechanics: new development and applications,” Ph.D dissertation, University of Oklahoma, Oklahoma, 1994.
- [3] Malik, M., Bert, C.W., “Differential quadrature analysis of free vibration of symmetric cross-ply laminates with shear deformation and rotatory inertia,” *Shock Vibr.*, Vol. 2, 1995, pp. 321–338.
- [4] Liew, K.M., Han, B., Xiao, M., “Differential quadrature method for thick symmetric cross-ply laminates with first-order shear flexibility,” *International Journal of Solids and Structures*, Vol. 33, 1996, pp. 2647–2658.
- [5] Davi, G., “Stress field in general composite laminates,” *American Institute of Aeronautics and Astronautics Journal*, Vol. 34, 1996, pp. 2604–2608.
- [6] Ferreira, A.J.M., Roque, C.C., Carrera, E., Cinefra, M., “Analysis of thick isotropic and cross-ply laminated plates by Radial Basis Functions and Unified Formulation,” *Journal of Sound and Vibration*, Vol. 330, 2011, pp. 771–787.
- [7] Ferreira, A.J.M., Roque, C.C., Carrera, E., Cinefra, M., Polit, O., “Analysis of laminated shells by a sinusoidal shear deformation theory and Radial Basis Functions collocation, accounting for through-the-thickness deformations,” *Composites Part B*, Vol. 42, 2011, pp. 1276–1284.
- [8] Ferreira, A.J.M., Roque, C.C., Carrera, E., Cinefra, M., “Analysis of laminated doubly-curved shells by a layer-wise theory and radial basis functions collocation, accounting for through-the-thickness deformations,” *Computational Mechanics*, Vol. 48(1), 2011, pp. 13–25.
- [9] Reddy, J.N., Robbins, D.H., “Theories and computational models for composite laminates,” *Applied Mechanics Review*, Vol. 47, 1994, pp. 147–165.
- [10] Varadan, T.K., Bhaskar, K., “Review of different theories for the the analysis of composites,” *Journal of Aerospace Society of India*, Vol. 49, 1997, pp. 202–208.
- [11] Carrera, E., “Developments, ideas and evaluations based upon Reissner’s Mixed Variational Theorem in the Modeling of Multilayered Plates and Shells,” *Applied Mechanics Review*, Vol. 54, 2001, pp. 301–329.
- [12] MacNeal, R.H., “Perspective on finite elements for shell analysis,” *Finite Elements in Analysis and Design*, Vol. 30, 1998, pp. 175–186.
- [13] Argyris, J.H., “Matrix displacement analysis of plates and shells, Prolegomena to a General Theory, Part I,” *Ingenieur-Archiv*, Vol. 35, 1966, pp. 102–142.
- [14] Sabir, A.B., Lock, A.C., “The application of finite elements to the large deflection geometrically non-linear behaviour of cylindrical shells,” *Variational Methods in Engineering 2*, (Eds. C.A. Brebbia, H. Tottenham). Southampton University Press 1972, 7/66-7/75.
- [15] Wempner, G.A., Oden, J.T., Kross, D.A., “Finite element analysis of thin shells,” *Journal of Engineering Mechanics ASCE* 94, Vol. 94, 1968, pp. 1273–1294.
- [16] Abel, J.F., Popov, E.P., “Static and dynamic finite element analysis of sandwich structures,” *Proceedings of the Second Conference of Matrix Methods in Structural Mechanics*, Vol. AFFSL-TR-68-150, 1968, pp. 213–245.

- [17] Monforton, G.R., Schmidt, L.A., "Finite element analyses of sandwich plates and cylindrical shells with laminated faces," *Proceedings of the Second Conference of Matrix Methods in Structural Mechanics*, Vol. AFFSL-TR-68-150, 1968, pp. 573–308.
- [18] Pryor, C.W., Barker, R.M., "A finite element analysis including transverse shear effect for applications to laminated plates," *American Institute of Aeronautics and Astronautics Journal*, Vol. 9, 1971, pp. 912–917.
- [19] Noor, A.K., "Finite Element Analysis of Anisotropic Plates," *American Institute of Aeronautics and Astronautics Journal*, Vol. 11, 1972, pp. 289–307.
- [20] Hughes, T.J.R., Tezduyar, T., "Finite elements based upon Mindlin plate theory with particular reference to the four-node isoparametric element," *Journal of Applied Mechanics*, Vol. 48, 1981, pp. 587–596.
- [21] Panda, S.C., Natarajan, R., "Finite Element Analysis of Laminated Composites Plates," *International Journal for Numerical Methods in Engineering*, Vol. 14, 1979, pp. 69–79.
- [22] Parisch, H., "A critical survey of the 9-node degenerated shell element with special emphasis on thin shell application and reduced integration," *Computer Methods in Applied Mechanics and Engineering*, Vol. 20, 1979, pp. 323–350.
- [23] Ferreira, A.J.M., Barbosa, J.T., Marques, A.T., De S, J.C., "Non-linear analysis of sandwich shells: the effect of core plasticity," *Computers & Structures*, Vol. 76, 2000, pp. 337–346.
- [24] Zienkiewicz, O.C., Taylor, R.L., Too, J.M., "Reduced intergration technique in general analysis of plates and shells," *International Journal for Numerical Methods in Engineering*, Vol. 3, 1973, pp. 275–290.
- [25] Chinosi, C., Lovadina, C., "Remarks on partial selective reduced integration method for Reissner-Mindlin plate problem," *Computers & Structures*, Vol. 73, 1999, pp. 73–78.
- [26] Pugh, E.D.L., Hintonand, E., Zienkiewicz, O.C., "A study of quadrilater plate bending elements with reduced integration," *International Journal for Numerical Methods in Engineering*, Vol. 12, 1978, pp. 1059–1079.
- [27] Hughes, T.J.R., Cohen, M., Horaun, M., "Reduced and selective integration techniques in the finite element methods," *Nuclear Engineering and Design*, Vol. 46, 1978, pp. 203–222.
- [28] Malkus, D.S., Hughes, T.J.R., "Mixed finite element methods - reduced and selective integration techniques: a unified concepts," *Computer Methods in Applied Mechanics and Engineering*, Vol. 15, 1978, pp. 63–81.
- [29] Chinosi, C., Della Croce, L., Scapolla, T., "Solving thin Naghdi shells with special finite elements," *Mathematical Modeling & Scientific Computing*, Vol. 8, 1997.
- [30] Chinosi, C., Della Croce, L., Scapolla, T., "Hierarchic finite elements for thin Naghdi shell model," *International Journal of Solids and Structures*, Vol. 35, No. 16, 1998, pp. 1863–1880.
- [31] Naghdi, P.M., "The theory of shells and plates," *Handbuch der Physic*, Vol. 4, 1972, pp. 425–640, Springer, Berlin.
- [32] Bathe, K.J., Dvorkin, E.N., "A four node plate bending element based on Mindlin/Reissner plate theory and mixed interpolation," *International Journal for Numerical Methods in Engineering*, Vol. 21, 1985, pp. 367–383.

- [33] Bathe, K.J., Brezzi, F., Cho, S.W., “The MITC7 and MITC9 plate elements,” *Computers and Structures*, Vol. 32, 1989, pp. 797–814.
- [34] Bathe, K.J., Brezzi, F., Fortin, M., “Mixed interpolated elements for Reissner-Mindlin plates,” *International Journal for Numerical Methods in Engineering*, Vol. 28, 1989, pp. 1787–1801.
- [35] Huang, N.C., Hinton, E., “A nine node Lagrangian Mindlin plate element with enhanced shear interpolation,” *Engineering Computations*, Vol. 1, 1984, pp. 369–379.
- [36] Auricchio, F., Sacco, L., “A mixed-enhanced finite elements for the analysis of laminated composites,” *International Journal for Numerical Methods in Engineering*, Vol. 44, 1999, pp. 1481–1504.
- [37] Brank, B., Carrera, E., “A Family of Shear-Deformable Shell Finite Elements for Composite Structures,” *Computer & Structures*, Vol. 76, 2000, pp. 297–297.
- [38] Arnold, D.N., Brezzi, F., “Locking-free finite element methods for shells,” *Mathematics of Computation*, Vol. 66, No. 217, 1997, pp. 1–14.
- [39] Büchter, N., Ramm, E., “3d-extension of non-linear shell equations based on the enhanced assumed strain concept,” *Computational Methods in Applied Sciences*, Hirsch C.(ed). Elsevier, 1992, pp. 55–62.
- [40] Bischoff, M., Ramm, E., “Shear-deformable shell elements for large strains and rotations,” *International Journal for Numerical Methods in Engineering*, Vol. 40, 1997, pp. 4427–4449.
- [41] Bischoff, M., Ramm, E., “On the physical significance of higher-order kinematic and static variables in a three-dimensional shell formulation,” *International Journal of Solids and Structures*, Vol. 37, 2000, pp. 6933–6960.
- [42] Bletzinger, K.U., Bischoff, M., Ramm, E., “A unified approach for shear-locking-free triangular and rectangular shell finite elements,” *Computers & Structures*, Vol. 75, 2000, pp. 321–334.
- [43] Braun, M., Bischoff, M., Ramm, E., “Non linear shell formulations for complete three-dimensional constitutive laws including composites and laminates,” *Computational Mechanics*, Vol. 15, 1994, pp. 1–18.
- [44] Simo, J.C., Rafai, S., “A class of mixed assumed strain methods and the method of incompatible modes,” *International Journal for Numerical Methods in Engineering*, Vol. 29, 1990, pp. 1595–1638.
- [45] Kant, T., Owen, D.R.J., Zienkiewicz, O.C., “Refined higher order C^0 plate bending element,” *Computer & Structures*, Vol. 15, 1982, pp. 177–183.
- [46] Kant, T., Kommineni, J.R., “Large Amplitude Free Vibration Analysis of Cross-Ply Composite and Sandwich Laminates with a Refined Theory and C^0 Finite Elements,” *Computer & Structures*, Vol. 50, 1989, pp. 123–134.
- [47] Dau, F., Polit, O., Touratier, M., “ C^1 plate and shell finite elements for geometrically nonlinear analysis of multilayered structures,” *Computer & Structures*, Vol. 84, 2006, pp. 1264–1274.
- [48] Dau, F., Polit, O., Touratier, M., “An efficient C^1 finite element with continuity requirements for multilayered/sandwich shell structures,” *Computer & Structures*, Vol. 82, 2004, pp. 1889–1899.
- [49] Polit, O., Touratier, M., “A multilayered/sandwich triangular finite element applied to linear and non-linear analyses,” *Composite Structures*, Vol. 58, 2002, pp. 121–128.

- [50] Polit, O., Touratier, M., "High-order triangular sandwich plate finite element for linear and non-linear analyses," *Computational Methods in Applied Mechanics and Engineering*, Vol. 185, 2000, pp. 305–324.
- [51] Polit, O., Touratier, M., "A new laminated triangular finite element assuring interface continuity for displacements and stresses," *Composite Structures*, Vol. 38, Issues 1-4, 1997, pp. 37–44.
- [52] Tessler, A., "A Higher-order plate theory with ideal finite element suitability," *Computer Methods in Applied Mechanics and Engineering*, Vol. 85, 1991, pp. 183–205.
- [53] Reddy, J.N., "Mechanics of Laminated Composite Plates and Shells," Theory and Analysis, CRC Press, 1997.
- [54] Palazotto, A.N., Dennis, S.T., "Nonlinear analysis of shell structures," AIAA Series, 1992.
- [55] Disciuvia, M., Cicorello, A., Dalle Mura, E., "A class of multilayered anisotropic plate elements including the effects of transverse shear deformability," *Proceedings of AIDAA Conference*, Torino, 1985, pp. 877–892.
- [56] Bekou, A., Touratier, M., "A Rectangular Finite Element for analysis composite multilayered shallow shells in static, vibration and buckling," *International Journal for Numerical Methods in Engineering*, Vol. 36, 1993, pp. 627–653.
- [57] Reissner, E., "On a certain mixed variational theorem and on laminated elastic shell theory," *Proceedings of the Euromech-Colloquium*, Vol. 219, 1986, pp. 17–27.
- [58] Rao, K.M., Meyer-Piening, H.R., "Analysis of thick laminated anisotropic composites plates by the finite element method," *Composite Structures*, Vol. 15, 1990, pp. 185–213.
- [59] Carrera, E., "A class of two-dimensional theories for anisotropic multilayered plates analysis," *Accademia delle Scienze di Torino, Memorie Scienze Fisiche*, 1995-1996, pp. 19–20, 1995, pp. 1–39.
- [60] Murakami, H., "Laminated composite plate theory with improved in-plane responses," *Journal of Applied Mechanics*, Vol. 53, 1986, pp. 661–666.
- [61] Brank, B., Carrera, E., "Multilayered Shell Finite Element with Interlaminar Continuous Shear Stresses: A Refinement of the Reissner-Mindlin Formulation," *International Journal for Numerical Methods in Engineering*, Vol. 48, 2000, pp. 843–874.
- [62] Noor, A.K., Burton, W.S., "Assessment of computational models for multi-layered composite shells," *Applied Mechanics Review*, Vol. 43, 1990, pp. 67–97.
- [63] Reddy, J.N., "An evaluation of equivalent single layer and layer-wise theories of composite laminates," *Composite Structures*, Vol. 25, 1993, pp. 21–35.
- [64] Mawenya, A.S., Davies, J.D., "Finite element bending analysis of multilayer plates," *International Journal for Numerical Methods in Engineering*, Vol. 8, 1974, pp. 215–225.
- [65] Pinsky, P.M., Kim, K.O., "A multi-director formulation for nonlinear elastic-viscoelastic layered shells," *Computers & Structures*, Vol. 24, 1986, pp. 901–913.
- [66] Chaudhuri, R.A., Seide, P., "An approximate method for prediction of transverse shear stresses in a laminated shell," *International Journal of Solids and Structures*, Vol. 23, 1987, pp. 1145–1161.

- [67] Rammerstorfer, F.G., Dörninger, K., Starlinger, A., “Composite and sandwich shells,” in [388], 1992, pp. 131–194.
- [68] Carrera, E., “Theories and finite elements for multilayered anisotropic composite plates and shells,” *Archives of Computational Methods in Engineering*, Vol. 9, 2002, pp. 87–140.
- [69] Carrera, E., “Theories and finite elements for multilayered plates and shells: a unified compact formulation with numerical assessment and benchmarking,” *Archives of Computational Methods in Engineering*, Vol. 10, No. 3, 2003, pp. 215–296.
- [70] Bathe, K.J., Lee, P.S., Hiller, J.F., “Towards improving the MITC9 shell element,” *Computers and Structures*, Vol. 81, 2003, pp. 477–489.
- [71] Chinosi, C., Della Croce, L., “Mixed-interpolated elements for thin shell,” *Communications in Numerical Methods in Engineering*, Vol. 14, 1998, pp. 1155–1170.
- [72] Huang, N.C., “Membrane locking and assumed strain shell elements,” *Computers and Structures*, Vol. 27, No. 5, 1987, pp. 671–677.
- [73] Panasz, P., Wisniewski, K., “Nine-node shell elements with 6 dofs/node based on two-level approximations. Part I Theory and linear tests,” *Finite Elements in Analysis and Design*, Vol. 44, 2008, pp. 784–796.
- [74] Koiter, W.T., “On the foundations of the linear theory of thin elastic shell,” *Proc. Kon. Nederl. Akad. Wetensch.*, Vol. 73, 1970, pp. 169–195.
- [75] Ciarlet, P.G., Gratie, L., “Another approach to linear shell theory and a new proof of Korn’s inequality on a surface,” *C. R. Acad. Sci. Paris, Ser. I*, Vol. 340, 2005, pp. 471–478.
- [76] N.N. Rogacheva, “*The theory of piezoelectric Shells and Plates*”, CRC Press, Boca Raton, Florida (USA), 1994.
- [77] Chapelle, D., Bathe, K.J., “The finite element analysis of shells.-Fundamentals,” Springer, Berlin, 2003.
- [78] Bathe, K.-J., Dvorkin, E., “A formulation of general shell elements - the use of mixed interpolation of tensorial components,” *International Journal for Numerical Methods in Engineering*, Vol. 22, 1986, pp. 697–722.
- [79] Bucalem, M.L., Bathe, K.-J., “Higher-order MITC general shell elements,” *International Journal for Numerical Methods in Engineering*, Vol. 36, 1993, pp. 3729–3754.
- [80] Huang, N.N., “Influence of shear correction factors in the higher-order shear deformation laminated shell theory,” *International Journal of Solids and Structures*, Vol. 31, 1994, pp. 1263–1277.
- [81] Shu, X.-P., “A refined theory of laminated shells with higher-order transverse shear deformation,” *International Journal of Solids and Structures*, Vol. 34, No. 6, 1997, pp. 673–683.
- [82] Giunta, G., Biscani, F., Belouettar, S., Carrera, E., “Hierarchical modelling of doubly curved laminated composite shells under distributed and localised loadings,” *Composites Part B: Engineering*, Vol. 42, No. 4, 2011, pp. 682–691.
- [83] Carrera, E., “Multilayered shell theories accounting for layerwise mixed description, Part 1: governing equations,” *AIAA Journal*, Vol. 37, No. 9, 1999, pp. 1107–1116.
- [84] Carrera, E., “Multilayered shell theories accounting for layerwise mixed description, Part 2: numerical evaluations,” *AIAA Journal*, Vol. 37, No. 9, 1999, pp. 1117–1124.

Appendix

In order to write the fundamental nucleus $\mathbf{K}^{k\tau sij}$ in compact form, the following integrals in the domain Ω_k are defined:

$$\left(W_{m1\,n1}^k; W_{m1\,n2}^k; W_{m2\,n1}^k; W_{m2\,n2}^k\right) = \int_{\Omega_k} (N_{m1}N_{n1}; N_{m1}N_{n2}; N_{m2}N_{n1}; N_{m2}N_{n2}) d\alpha_k d\beta_k \quad (27)$$

$$\left(W_{m1\,n3}^k; W_{m3\,n1}^k; W_{m3\,n3}^k; W_{m2\,n3}^k; W_{m3\,n2}^k\right) = \int_{\Omega_k} (N_{m1}N_{n3}; N_{m3}N_{n1}; N_{m3}N_{n3}; N_{m2}N_{n3}; N_{m3}N_{n2}) d\alpha_k d\beta_k \quad (28)$$

$$\left(W_{m1\,j}^k; W_{m2\,j}^k; W_{m3\,j}^k\right) = \int_{\Omega_k} (N_{m1}N_j; N_{m2}N_j; N_{m3}N_j) d\alpha_k d\beta_k \quad (29)$$

$$\left(W_{i\,n1}^k; W_{i\,n2}^k; W_{i\,n3}^k; W_{i\,j}^k\right) = \int_{\Omega_k} (N_iN_{n1}; N_iN_{n2}; N_iN_{n3}; N_iN_j) d\alpha_k d\beta_k \quad (30)$$

$$\left(W_{m1\,j,\alpha}^k; W_{m1\,j,\beta}^k; W_{m2\,j,\alpha}^k; W_{m2\,j,\beta}^k\right) = \int_{\Omega_k} \left(N_{m1} \frac{\partial N_j}{\partial \alpha}; N_{m1} \frac{\partial N_j}{\partial \beta}; N_{m2} \frac{\partial N_j}{\partial \alpha}; N_{m2} \frac{\partial N_j}{\partial \beta}\right) d\alpha_k d\beta_k \quad (31)$$

$$\left(W_{i,\alpha\,n1}^k; W_{i,\beta\,n1}^k; W_{i,\alpha\,n2}^k; W_{i,\beta\,n2}^k\right) = \int_{\Omega_k} \left(\frac{\partial N_i}{\partial \alpha} N_{n1}; \frac{\partial N_i}{\partial \beta} N_{n1}; \frac{\partial N_i}{\partial \alpha} N_{n2}; \frac{\partial N_i}{\partial \beta} N_{n2}\right) d\alpha_k d\beta_k \quad (32)$$

Moreover, the integrals on the domain A_k , in the thickness direction, are written as:

$$\left(J^{k\tau s}, J_{\alpha}^{k\tau s}, J_{\beta}^{k\tau s}, J_{\frac{\alpha}{\beta}}^{k\tau s}, J_{\frac{\beta}{\alpha}}^{k\tau s}, J_{\alpha\beta}^{k\tau s}\right) = \int_{A_k} F_{\tau} F_s \left(1, H_{\alpha}^k, H_{\beta}^k, \frac{H_{\alpha}^k}{H_{\beta}^k}, \frac{H_{\beta}^k}{H_{\alpha}^k}, H_{\alpha}^k H_{\beta}^k\right) dz \quad (33)$$

$$\left(J^{k\tau_z s}, J_{\alpha}^{k\tau_z s}, J_{\beta}^{k\tau_z s}, J_{\frac{\alpha}{\beta}}^{k\tau_z s}, J_{\frac{\beta}{\alpha}}^{k\tau_z s}, J_{\alpha\beta}^{k\tau_z s}\right) = \int_{A_k} \frac{\partial F_{\tau}}{\partial z} F_s \left(1, H_{\alpha}^k, H_{\beta}^k, \frac{H_{\alpha}^k}{H_{\beta}^k}, \frac{H_{\beta}^k}{H_{\alpha}^k}, H_{\alpha}^k H_{\beta}^k\right) dz \quad (34)$$

$$\left(J^{k\tau s_z}, J_{\alpha}^{k\tau s_z}, J_{\beta}^{k\tau s_z}, J_{\frac{\alpha}{\beta}}^{k\tau s_z}, J_{\frac{\beta}{\alpha}}^{k\tau s_z}, J_{\alpha\beta}^{k\tau s_z} \right) = \int_{A_k} F_{\tau} \frac{\partial F_s}{\partial z} \left(1, H_{\alpha}^k, H_{\beta}^k, \frac{H_{\alpha}^k}{H_{\beta}^k}, \frac{H_{\beta}^k}{H_{\alpha}^k}, H_{\alpha}^k H_{\beta}^k \right) dz \quad (35)$$

$$\left(J^{k\tau_z s_z}, J_{\alpha}^{k\tau_z s_z}, J_{\beta}^{k\tau_z s_z}, J_{\frac{\alpha}{\beta}}^{k\tau_z s_z}, J_{\frac{\beta}{\alpha}}^{k\tau_z s_z}, J_{\alpha\beta}^{k\tau_z s_z} \right) = \int_{A_k} \frac{\partial F_{\tau}}{\partial z} \frac{\partial F_s}{\partial z} \left(1, H_{\alpha}^k, H_{\beta}^k, \frac{H_{\alpha}^k}{H_{\beta}^k}, \frac{H_{\beta}^k}{H_{\alpha}^k}, H_{\alpha}^k H_{\beta}^k \right) dz \quad (36)$$

The fundamental nucleus $\mathbf{K}^{k\tau sij}$ is a (3×3) matrix and the explicit expression of its components is:

$$\begin{aligned} K_{\alpha\alpha}^{k\tau sij} &= C_{55}^k N_i^{(m1)} N_j^{(n1)} W_{m1n1}^k J_{\alpha\beta}^{k\tau_z s_z} - \frac{C_{55}^k}{R_{\alpha}^k} N_i^{(m1)} N_j^{(n1)} W_{m1n1}^k J_{\beta}^{k\tau_z s} - \frac{C_{55}^k}{R_{\alpha}^k} N_i^{(m1)} N_j^{(n1)} W_{m1n1}^k J_{\beta}^{k\tau s_z} + \\ &+ C_{66}^k N_{i,\beta}^{(m3)} N_{j,\beta}^{(n3)} W_{m3n3}^k J_{\frac{\alpha}{\beta}}^{k\tau s} + C_{16}^k N_{i,\alpha}^{(m1)} N_{j,\beta}^{(n3)} W_{m1n3}^k J^{k\tau s} + C_{16}^k N_{i,\beta}^{(m3)} N_{j,\alpha}^{(n1)} W_{m3n1}^k J^{k\tau s} + \\ &+ C_{11}^k N_{i,\alpha}^{(m1)} N_{j,\alpha}^{(n1)} W_{m1n1}^k J_{\frac{\beta}{\alpha}}^{k\tau s} + \frac{C_{55}^k}{(R_{\alpha}^k)^2} N_i^{(m1)} N_j^{(n1)} W_{m1n1}^k J_{\frac{\beta}{\alpha}}^{k\tau s} \end{aligned} \quad (37)$$

$$\begin{aligned} K_{\alpha\beta}^{k\tau sij} &= C_{45}^k N_i^{(m1)} N_j^{(n2)} W_{m1n2}^k J_{\alpha\beta}^{k\tau_z s_z} - \frac{C_{45}^k}{R_{\beta}^k} N_i^{(m1)} N_j^{(n2)} W_{m1n2}^k J_{\alpha}^{k\tau_z s} - \frac{C_{45}^k}{R_{\alpha}^k} N_i^{(m1)} N_j^{(n2)} W_{m1n2}^k J_{\beta}^{k\tau s_z} + \\ &+ C_{26}^k N_{i,\beta}^{(m3)} N_{j,\beta}^{(n2)} W_{m3n2}^k J_{\frac{\alpha}{\beta}}^{k\tau s} + C_{12}^k N_{i,\alpha}^{(m1)} N_{j,\beta}^{(n2)} W_{m1n2}^k J^{k\tau s} + C_{66}^k N_{i,\beta}^{(m3)} N_{j,\alpha}^{(n3)} W_{m3n3}^k J^{k\tau s} + \\ &+ C_{16}^k N_{i,\alpha}^{(m1)} N_{j,\alpha}^{(n3)} W_{m1n3}^k J_{\frac{\beta}{\alpha}}^{k\tau s} + \frac{C_{45}^k}{R_{\alpha}^k R_{\beta}^k} N_i^{(m1)} N_j^{(n2)} W_{m1n2}^k J^{k\tau s} \end{aligned} \quad (38)$$

$$\begin{aligned} K_{\alpha z}^{k\tau sij} &= C_{45}^k N_i^{(m1)} N_{j,\beta}^{(n2)} W_{m1n2}^k J_{\alpha}^{k\tau_z s} + C_{55}^k N_i^{(m1)} N_{j,\alpha}^{(n1)} W_{m1n1}^k J_{\beta}^{k\tau_z s} + C_{36}^k N_{i,\beta}^{(m3)} W_{m3j}^k J_{\alpha}^{k\tau s_z} + \\ &+ C_{13}^k N_{i,\alpha}^{(m1)} W_{m1j}^k J_{\beta}^{k\tau s_z} - \frac{C_{45}^k}{R_{\alpha}^k} N_i^{(m1)} N_{j,\beta}^{(n2)} W_{m1n2}^k J^{k\tau s} - \frac{C_{55}^k}{R_{\alpha}^k} N_i^{(m1)} N_{j,\alpha}^{(n1)} W_{m1n1}^k J_{\frac{\beta}{\alpha}}^{k\tau s} + \\ &+ \frac{C_{26}^k}{R_{\beta}^k} N_{i,\beta}^{(m3)} N_j^{(n2)} W_{m3n2}^k J_{\frac{\alpha}{\beta}}^{k\tau s} + \frac{C_{16}^k}{R_{\alpha}^k} N_{i,\beta}^{(m3)} N_j^{(n1)} W_{m3n1}^k J^{k\tau s} + \frac{C_{12}^k}{R_{\beta}^k} N_{i,\alpha}^{(m1)} N_j^{(n2)} W_{m1n2}^k J^{k\tau s} + \\ &+ \frac{C_{11}^k}{R_{\alpha}^k} N_{i,\alpha}^{(m1)} N_j^{(n1)} W_{m1n1}^k J_{\frac{\beta}{\alpha}}^{k\tau s} \end{aligned} \quad (39)$$

$$\begin{aligned}
K_{\beta\alpha}^{k\tau sij} = & C_{45}^k N_i^{(m2)} N_j^{(n1)} W_{m2\,n1}^k J_{\alpha\beta}^{k\tau_z s_z} - \frac{C_{45}^k}{R_\alpha^k} N_i^{(m2)} N_j^{(n1)} W_{m2\,n1}^k J_\beta^{k\tau_z s} - \frac{C_{45}^k}{R_\beta^k} N_i^{(m2)} N_j^{(n1)} W_{m2\,n1}^k J_\alpha^{k\tau s_z} + \\
& + C_{26}^k N_{i,\beta}^{(m2)} N_{j,\beta}^{(n3)} W_{m2\,n3}^k J_{\frac{\alpha}{\beta}}^{k\tau s} + C_{66}^k N_{i,\alpha}^{(m3)} N_{j,\beta}^{(n3)} W_{m3\,n3}^k J^{k\tau s} + C_{12}^k N_{i,\beta}^{(m2)} N_{j,\alpha}^{(n1)} W_{m2\,n1}^k J^{k\tau s} + \\
& + C_{16}^k N_{i,\alpha}^{(m3)} N_{j,\alpha}^{(n1)} W_{m3\,n1}^k J_{\frac{\beta}{\alpha}}^{k\tau s} + \frac{C_{45}^k}{R_\alpha^k R_\beta^k} N_i^{(m2)} N_j^{(n1)} W_{m2\,n1}^k J^{k\tau s}
\end{aligned} \tag{40}$$

$$\begin{aligned}
K_{\beta\beta}^{k\tau sij} = & C_{44}^k N_i^{(m2)} N_j^{(n2)} W_{m2\,n2}^k J_{\alpha\beta}^{k\tau_z s_z} - \frac{C_{44}^k}{R_\beta^k} N_i^{(m2)} N_j^{(n2)} W_{m2\,n2}^k J_\alpha^{k\tau_z s} - \frac{C_{44}^k}{R_\beta^k} N_i^{(m2)} N_j^{(n2)} W_{m2\,n2}^k J_\alpha^{k\tau s_z} + \\
& + C_{22}^k N_{i,\beta}^{(m2)} N_{j,\beta}^{(n2)} W_{m2\,n2}^k J_{\frac{\alpha}{\beta}}^{k\tau s} + C_{26}^k N_{i,\alpha}^{(m3)} N_{j,\beta}^{(n2)} W_{m3\,n2}^k J^{k\tau s} + C_{26}^k N_{i,\beta}^{(m2)} N_{j,\alpha}^{(n3)} W_{m2\,n3}^k J^{k\tau s} + \\
& + C_{66}^k N_{i,\alpha}^{(m3)} N_{j,\alpha}^{(n3)} W_{m3\,n3}^k J_{\frac{\beta}{\alpha}}^{k\tau s} + \frac{C_{44}^k}{(R_\beta^k)^2} N_i^{(m2)} N_j^{(n2)} W_{m2\,n2}^k J_{\frac{\alpha}{\beta}}^{k\tau s}
\end{aligned} \tag{41}$$

$$\begin{aligned}
K_{\beta z}^{k\tau sij} = & C_{44}^k N_i^{(m2)} N_{j,\beta}^{(n2)} W_{m2\,n2}^k J_\alpha^{k\tau_z s} + C_{45}^k N_i^{(m2)} N_{j,\alpha}^{(n1)} W_{m2\,n1}^k J_\beta^{k\tau_z s} + C_{23}^k N_{i,\beta}^{(m2)} W_{m2\,j}^k J_\alpha^{k\tau s_z} + \\
& + C_{36}^k N_{i,\alpha}^{(m3)} W_{m3\,j}^k J_\beta^{k\tau s_z} - \frac{C_{44}^k}{R_\beta^k} N_i^{(m2)} N_{j,\beta}^{(n2)} W_{m2\,n2}^k J_{\frac{\alpha}{\beta}}^{k\tau s} - \frac{C_{45}^k}{R_\beta^k} N_i^{(m2)} N_{j,\alpha}^{(n1)} W_{m2\,n1}^k J^{k\tau s} + \\
& + \frac{C_{22}^k}{R_\beta^k} N_{i,\beta}^{(m2)} N_j^{(n2)} W_{m2\,n2}^k J_{\frac{\alpha}{\beta}}^{k\tau s} + \frac{C_{12}^k}{R_\alpha^k} N_{i,\beta}^{(m2)} N_j^{(n1)} W_{m2\,n1}^k J^{k\tau s} + \frac{C_{26}^k}{R_\beta^k} N_{i,\alpha}^{(m3)} N_j^{(n2)} W_{m3\,n2}^k J^{k\tau s} + \\
& + \frac{C_{16}^k}{R_\alpha^k} N_{i,\alpha}^{(m3)} N_j^{(n1)} W_{m3\,n1}^k J_{\frac{\beta}{\alpha}}^{k\tau s}
\end{aligned} \tag{42}$$

$$\begin{aligned}
K_{z\alpha}^{k\tau sij} = & C_{36}^k N_{j,\beta}^{(n3)} W_{i\,n3}^k J_\alpha^{k\tau_z s} + C_{13}^k N_{j,\alpha}^{(n1)} W_{i\,n1}^k J_\beta^{k\tau_z s} + C_{45}^k N_{i,\beta}^{(m2)} N_j^{(n1)} W_{m2\,n1}^k J_\alpha^{k\tau s_z} + \\
& + C_{55}^k N_{i,\alpha}^{(m1)} N_j^{(n1)} W_{m1\,n1}^k J_\beta^{k\tau s_z} + \frac{C_{26}^k}{R_\beta^k} N_i^{(m2)} N_{j,\beta}^{(n3)} W_{m2\,n3}^k J_{\frac{\alpha}{\beta}}^{k\tau s} + \frac{C_{16}^k}{R_\alpha^k} N_i^{(m1)} N_{j,\beta}^{(n3)} W_{m1\,n3}^k J^{k\tau s} + \\
& + \frac{C_{12}^k}{R_\beta^k} N_i^{(m2)} N_{j,\alpha}^{(n1)} W_{m2\,n1}^k J^{k\tau s} + \frac{C_{11}^k}{R_\alpha^k} N_i^{(m1)} N_{j,\alpha}^{(n1)} W_{m1\,n1}^k J_{\frac{\beta}{\alpha}}^{k\tau s} - \frac{C_{45}^k}{R_\alpha^k} N_{i,\beta}^{(m2)} N_j^{(n1)} W_{m2\,n1}^k J^{k\tau s} - \\
& - \frac{C_{55}^k}{R_\alpha^k} N_{i,\alpha}^{(m1)} N_j^{(n1)} W_{m1\,n1}^k J_{\frac{\beta}{\alpha}}^{k\tau s}
\end{aligned} \tag{43}$$

$$\begin{aligned}
K_{z\beta}^{k\tau sij} = & C_{23}^k N_{j,\beta}^{(n2)} W_{i n 2}^k J_{\alpha}^{k\tau z s} + C_{36}^k N_{j,\alpha}^{(n3)} W_{i n 3}^k J_{\beta}^{k\tau z s} + C_{44}^k N_{i,\beta}^{(m2)} N_j^{(n2)} W_{m 2 n 2}^k J_{\alpha}^{k\tau s z} + \\
& + C_{45}^k N_{i,\alpha}^{(m1)} N_j^{(n2)} W_{m 1 n 2}^k J_{\beta}^{k\tau s z} + \frac{C_{22}^k}{R_{\beta}^k} N_i^{(m2)} N_{j,\beta}^{(n2)} W_{m 2 n 2}^k J_{\frac{\alpha}{\beta}}^{k\tau s} + \frac{C_{12}^k}{R_{\alpha}^k} N_i^{(m1)} N_{j,\beta}^{(n2)} W_{m 1 n 2}^k J^{k\tau s} + \\
& + \frac{C_{26}^k}{R_{\beta}^k} N_i^{(m2)} N_{j,\alpha}^{(n3)} W_{m 2 n 3}^k J^{k\tau s} + \frac{C_{16}^k}{R_{\alpha}^k} N_i^{(m1)} N_{j,\alpha}^{(n3)} W_{m 1 n 3}^k J_{\frac{\beta}{\alpha}}^{k\tau s} - \frac{C_{44}^k}{R_{\beta}^k} N_{i,\beta}^{(m2)} N_j^{(n2)} W_{m 2 n 2}^k J_{\frac{\alpha}{\beta}}^{k\tau s} - \\
& - \frac{C_{45}^k}{R_{\beta}^k} N_{i,\alpha}^{(m1)} N_j^{(n2)} W_{m 1 n 2}^k J^{k\tau s}
\end{aligned} \tag{44}$$

$$\begin{aligned}
K_{zz}^{k\tau sij} = & C_{33}^k W_{ij}^k J_{\alpha\beta}^{k\tau z s z} + \frac{C_{23}^k}{R_{\beta}^k} N_j^{(n2)} W_{i n 2}^k J_{\alpha}^{k\tau z s} + \frac{C_{13}^k}{R_{\alpha}^k} N_j^{(n1)} W_{i n 1}^k J_{\beta}^{k\tau z s} + \\
& + \frac{C_{23}^k}{R_{\beta}^k} N_i^{(m2)} W_{m 2 j}^k J_{\alpha}^{k\tau s z} + \frac{C_{13}^k}{R_{\alpha}^k} N_i^{(m1)} W_{m 1 j}^k J_{\beta}^{k\tau s z} + C_{44}^k N_{i,\beta}^{(m2)} N_{j,\beta}^{(n2)} W_{m 2 n 2}^k J_{\frac{\alpha}{\beta}}^{k\tau s} + \\
& + C_{45}^k N_{i,\alpha}^{(m1)} N_{j,\beta}^{(n2)} W_{m 1 n 2}^k J^{k\tau s} + C_{45}^k N_{i,\beta}^{(m2)} N_{j,\alpha}^{(n1)} W_{m 2 n 1}^k J^{k\tau s} + C_{55}^k N_{i,\alpha}^{(m1)} N_{j,\alpha}^{(n1)} W_{m 1 n 1}^k J_{\frac{\beta}{\alpha}}^{k\tau s} + \\
& + \frac{C_{12}^k}{R_{\alpha}^k R_{\beta}^k} N_i^{(m1)} N_j^{(n2)} W_{m 1 n 2}^k J^{k\tau s} + \frac{C_{12}^k}{R_{\alpha}^k R_{\beta}^k} N_i^{(m2)} N_j^{(n1)} W_{m 2 n 1}^k J^{k\tau s} + \\
& + \frac{C_{22}^k}{(R_{\beta}^k)^2} N_i^{(m2)} N_j^{(n2)} W_{m 2 n 2}^k J_{\frac{\alpha}{\beta}}^{k\tau s} + \frac{C_{11}^k}{(R_{\alpha}^k)^2} N_i^{(m1)} N_j^{(n1)} W_{m 1 n 1}^k J_{\frac{\beta}{\alpha}}^{k\tau s}
\end{aligned} \tag{45}$$

Table 1: Elastic and Geometrical properties

<i>Spherical panel</i>	
E_{11}/E_{22}	25
$G_{12}/E_{22} = G_{13}/E_{22}$	0.5
G_{23}/E_{22}	0.2
$\nu_{12} = \nu_{13} = \nu_{23}$	0.25
\hat{p}_z^+	1
m, n	1,1

Table 2: Transversal displacement $\bar{w}(z = 0)$. Symmetric lamination $(0^\circ, 90^\circ, 0^\circ)$.

	$R/a = 1$			$R/a = 2$			$R/a = 5$		
3D [80]	—	—	—	1.482	0.6087	—	1.549	0.7325	—
HS DT_1 [81]	1.208	0.3761	—	1.482	0.6090	—	1.546	0.7340	—
L4 _a	1.2081	0.3766	0.0054	1.4824	0.6087	0.0208	1.5494	0.7325	0.1036
a/h	5	10	100	5	10	100	5	10	100
L4	1.2081	0.3767	0.0054	1.4824	0.6087	0.0208	1.5494	0.7325	0.1036
L1	1.1839	0.3732	0.0054	1.4413	0.5990	0.0208	1.5019	0.7179	0.1036
EZ3	1.2015	0.3760	0.0054	1.4772	0.6081	0.0208	1.5452	0.7322	0.1036
E4	1.1656	0.3693	0.0054	1.4038	0.5858	0.0208	1.4564	0.6974	0.1036
E2	1.0342	0.3504	0.0054	1.1776	0.5315	0.0208	1.1961	0.6174	0.1036
FSDT	1.0491	0.3507	0.0054	1.1968	0.5326	0.0208	1.2129	0.6191	0.1036
CLT	0.5148	0.2947	0.0054	0.4748	0.3934	0.0208	0.4487	0.4295	0.1034

Table 3: Transversal displacement $\bar{w}(z = 0)$. Antisymmetric lamination $(0^\circ, 90^\circ, 0^\circ, 90^\circ)$.

	$R/a = 1$			$R/a = 2$			$R/a = 5$		
3D [80]	—	—	—	1.434	0.6128	—	1.495	0.7408	—
HS DT_1 [81]	1.179	0.3748	—	1.433	0.6085	—	1.488	0.7345	—
L4 _a	1.1768	0.3763	0.0054	1.4344	0.6128	0.0208	1.4951	0.7408	0.1067
a/h	5	10	100	5	10	100	5	10	100
L4	1.1769	0.3763	0.0054	1.4343	0.6128	0.0208	1.4951	0.7408	0.1067
EZ3	1.1650	0.3746	0.0054	1.4152	0.6079	0.0208	1.4733	0.7333	0.1067
E4	1.1190	0.3689	0.0054	1.3295	0.5899	0.0208	1.3719	0.7054	0.1067
FSDT	0.9943	0.3543	0.0054	1.1096	0.5452	0.0208	1.1154	0.6383	0.1067
CLT	0.5823	0.3173	0.0054	0.5522	0.4478	0.0208	0.5261	0.5016	0.1066

Table 4: Transversal displacement $\bar{w}(z = 0)$. Symmetric lamination $(0^\circ, 90^\circ, 0^\circ, 90^\circ, 0^\circ)$.

	$R/a = 1$			$R/a = 2$			$R/a = 5$		
3D [80]	—	—	—	1.376	0.5671	—	1.417	0.6707	—
HSDT ₁ [81]	1.151	0.3615	—	1.379	0.5670	—	1.425	0.6708	—
L4 _a	1.1397	0.3617	0.0054	1.3674	0.5671	0.0207	1.4165	0.6707	0.1032
a/h	5	10	100	5	10	100	5	10	100
L4	1.1397	0.3617	0.0054	1.3674	0.5671	0.0207	1.4165	0.6706	0.1032
EZ3	1.1315	0.3608	0.0054	1.3543	0.5647	0.0207	1.4017	0.6672	0.1032
E4	1.0476	0.3504	0.0054	1.2052	0.5341	0.0207	1.2286	0.6219	0.1032
FSDT	0.9794	0.3413	0.0054	1.0873	0.5090	0.0207	1.0910	0.5862	0.1032
CLT	0.5133	0.2937	0.0054	0.4744	0.3929	0.0207	0.4486	0.4294	0.1031

Table 5: In-plane stress $\bar{\sigma}_{\alpha\alpha}(z = -h/2)$. Symmetric lamination $(0^\circ, 90^\circ, 0^\circ)$.

	$R/a = 1$			$R/a = 2$			$R/a = 5$		
HSDT ₁ [81]	-0.4699	—	—	-0.6706	—	—	-0.7399	—	—
L4 _a	-0.5080	-0.2362	0.0012	-0.6740	-0.4433	-0.0112	-0.7128	-0.5616	-0.1003
a/h	5	10	100	5	10	100	5	10	100
L4	-0.5055	-0.2351	0.0012	-0.6706	-0.4411	-0.0112	-0.7092	-0.5588	-0.0999
L1	-0.4579	-0.2300	0.0012	-0.6079	-0.4291	-0.0112	-0.6432	-0.5415	-0.1001
EZ3	-0.5042	-0.2355	0.0012	-0.6692	-0.4415	-0.0112	-0.7080	-0.5593	-0.0999
E4	-0.5144	-0.2418	0.0012	-0.6661	-0.4433	-0.0112	-0.6972	-0.5543	-0.0999
E2	-0.3464	-0.2306	0.0012	-0.4446	-0.4048	-0.0112	-0.4644	-0.4938	-0.1000
FSDT	-0.3592	-0.2293	0.0012	-0.4569	-0.4037	-0.0112	-0.4769	-0.4941	-0.1000
CLT	-0.6317	-0.3149	0.0012	-0.6031	-0.4681	-0.0114	-0.5659	-0.5281	-0.1005

Table 6: Shear stress $\bar{\sigma}_{\alpha z}$ evaluated in ($z = 0$) for $N_l = 3, 5$ and ($z = -h/8$) for $N_l = 4$. Curvature ratio $R/a = 2$.

	$N_l = 3$			$N_l = 4$			$N_l = 5$		
L4 _a	0.2744	0.2821	0.0184	0.2380	0.2090	0.0077	0.2654	0.2378	0.0145
a/h	5	10	100	5	10	100	5	10	100
L4	0.2771	0.2849	0.0186	0.2168	0.1663	0.0112	0.2681	0.2401	0.0146
L1	0.2791	0.2863	0.0186	0.1972	0.1557	0.0107	0.2590	0.2351	0.0143
EZ3	0.2787	0.2881	0.0188	0.2005	0.1587	0.0113	0.2729	0.2487	0.0153
E4	0.2175	0.2114	0.0132	0.2508	0.2040	0.0146	0.4335	0.4570	0.1176
E2	0.1266	0.1145	0.0067	0.2211	0.1826	0.0138	0.2740	0.2509	0.0148
FSDT	0.1270	0.1141	0.0067	0.2363	0.1977	0.0141	0.2752	0.2502	0.0147

Table 7: Antisymmetric lamination ($45^\circ / -45^\circ$) with simply-supported boundary conditions and bi-sinusoidal load. Theory L4.

	$R/a = 1$			$R/a = 2$			$R/a = 5$		
a/h	5	10	100	5	10	100	5	10	100
w	0.4476	0.1115	0.0009	0.8614	0.3017	0.0036	1.1633	0.5738	0.0236
$\sigma_{\alpha\alpha}$	0.1917	0.0819	0.0051	0.2881	0.1693	0.0101	0.3256	0.2547	0.0308
	0.0025	0.0238	0.0047	-0.1040	-0.0260	0.0086	-0.2190	-0.1443	0.0164
$\sigma_{\beta\beta}$	0.1917	0.0819	0.0051	0.2881	0.1693	0.0101	0.3256	0.2547	0.0308
	0.0025	0.0238	0.0047	-0.1040	-0.0260	0.0086	-0.2190	-0.1443	0.0164
$\sigma_{\alpha\beta}$	-0.0154	-0.0120	-0.0017	-0.0473	-0.0415	-0.0115	-0.0722	-0.0723	-0.0476
	1.0585	0.5024	0.0308	1.3171	0.7804	0.0726	1.1315	0.8170	0.2007
$\sigma_{\alpha z}$	0.1074	0.0766	0.0081	0.1761	0.1628	0.0207	0.2220	0.2727	0.0780
$\sigma_{\beta z}$	0.0967	0.0641	0.0019	0.1651	0.1427	0.0052	0.2168	0.2563	0.0290
σ_{zz}	0.5515	0.5720	0.6319	0.5061	0.4884	0.7049	0.5296	0.4886	0.9962

Table 8: Symmetric lamination ($0^\circ/90^\circ/0^\circ$) with clamped-free boundary conditions and bi-sinusoidal load. Theory L4.

	$R/a = 1$			$R/a = 2$			$R/a = 5$		
a/h	5	10	100	5	10	100	5	10	100
w	0.3119	0.0819	0.0013	0.6495	0.1936	0.0042	1.0508	0.3618	0.0190
$\sigma_{\alpha\alpha}$	0.3731	0.1748	0.0166	0.5077	0.2787	0.0359	0.5627	0.3530	0.0929
	0.0531	0.0326	0.0069	-0.0206	-0.0032	0.0099	-0.2283	-0.1378	0.0058
$\sigma_{\beta\beta}$	0.0252	0.0082	0.0004	0.0353	0.0138	0.0008	0.0434	0.0206	0.0022
	-0.0084	-0.0024	0.0002	-0.0192	-0.0077	0.0001	-0.0296	-0.0155	-0.0006
$\sigma_{\alpha\beta}$	0.0020	0.0006	-0.0003	0.0007	0.0007	0.0000	-0.0049	-0.0021	0.0006
	0.0090	0.0029	-0.0002	0.0155	0.0065	0.0002	0.0170	0.0085	0.0009
$\sigma_{\alpha z}$	-0.0015	-0.0188	-0.0618	0.1363	0.1078	-0.0681	0.2923	0.2986	-0.0126
$\sigma_{\beta z}$	-0.0009	-0.0025	-0.0020	0.0011	-0.0008	-0.0019	0.0033	0.0014	-0.0016
σ_{zz}	0.6672	0.6347	0.6140	0.6986	0.6565	0.5755	0.7532	0.7381	0.5398

Table 9: Symmetric lamination ($90^\circ/0^\circ/90^\circ$) with simply-supported boundary conditions and concentrated load. Theory L4.

	$R/a = 1$			$R/a = 2$			$R/a = 5$		
a/h	5	10	100	5	10	100	5	10	100
w	35.5844	3.2329	0.0012	43.3005	4.5602	0.0027	46.4546	5.3029	0.0083
$\sigma_{\alpha\alpha}$	24.6050	1.9587	0.0016	26.7568	2.1125	0.0023	28.0121	2.1866	0.0034
	-2.8433	-0.5929	-0.0012	-3.4302	-0.7221	-0.0018	-3.6722	-0.7921	-0.0029
$\sigma_{\beta\beta}$	129.4768	11.3214	0.0186	138.6554	12.4595	0.0243	143.2570	12.9911	0.0334
	-22.2940	-4.5605	-0.0108	-26.8411	-5.8998	-0.0153	-28.5773	-6.6941	-0.0239
$\sigma_{\alpha\beta}$	0.2677	0.0688	0.0001	-0.0895	0.0261	0.0002	-0.4274	-0.0471	0.0005
	1.1584	0.1536	0.0001	1.0927	0.1823	0.0003	0.8786	0.1542	0.0007
$\sigma_{\alpha z}$	0.8085	0.0831	0.0003	0.7397	0.0770	0.0004	0.5528	0.0449	0.0004
$\sigma_{\beta z}$	1.9680	0.2951	-0.0013	3.2534	0.7891	-0.0037	3.7429	1.0684	-0.0017
σ_{zz}	4.7550	2.0643	0.0255	4.9643	2.1359	0.0262	5.1002	2.1881	0.0268

Figures

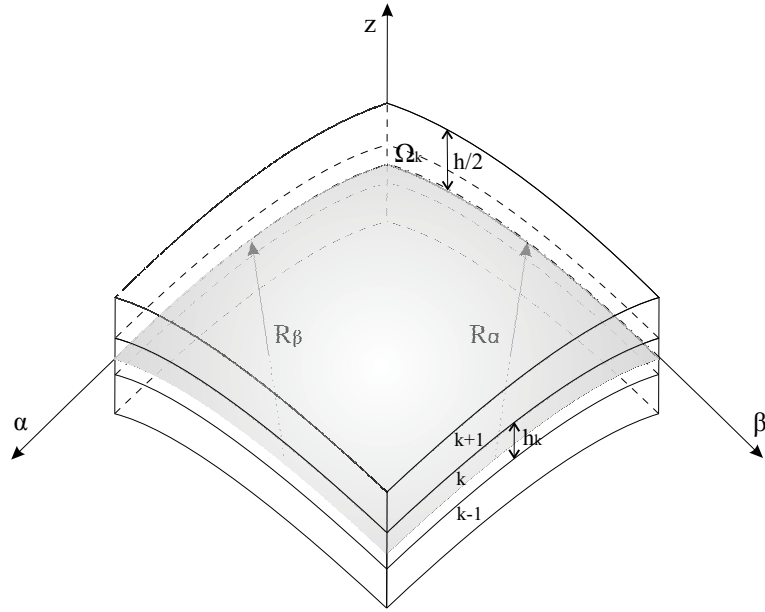


Figure 1: Multilayered doubly-curved shell: notation and geometry.

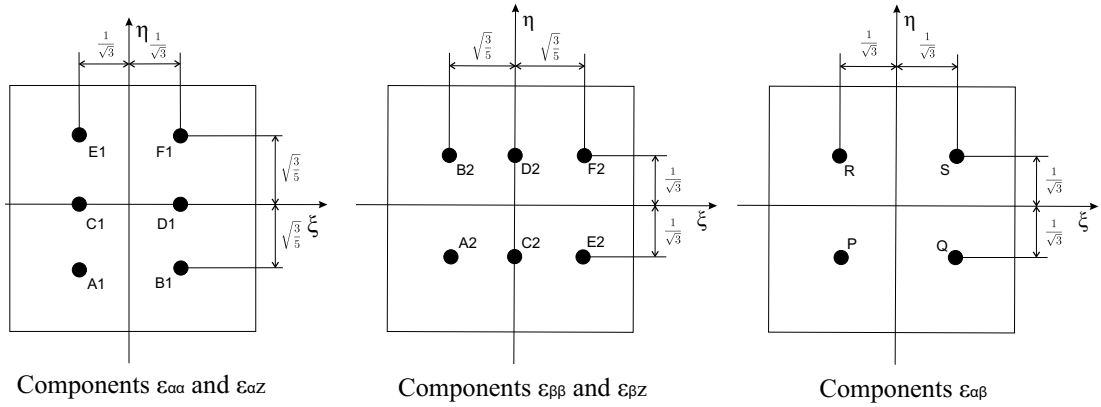


Figure 2: Tying points for the MITC9 shell element.

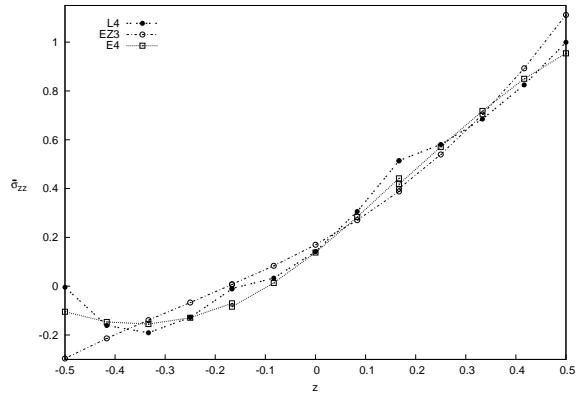
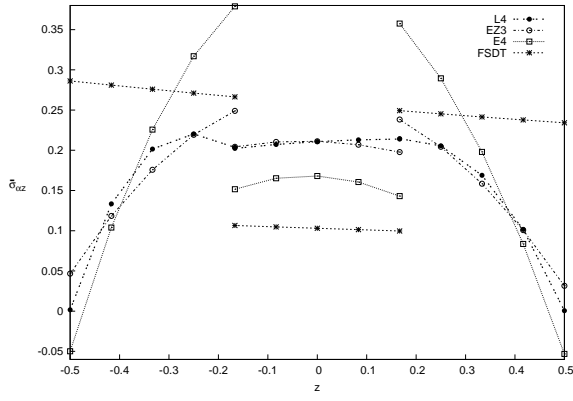


Figure 3: Shear stress $\bar{\sigma}_{\alpha z}$, $R/a = 1$ and Figure 4: Normal stress $\bar{\sigma}_{zz}$. $R/a = 1$ and $a/h = 5$. Symmetric lamination with $N_l = 3$. $a/h = 5$. Symmetric lamination with $N_l = 3$.

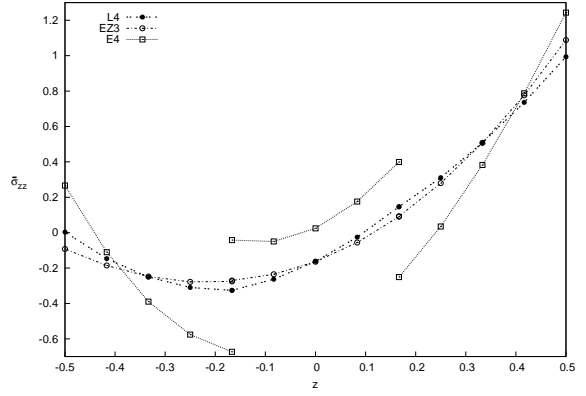
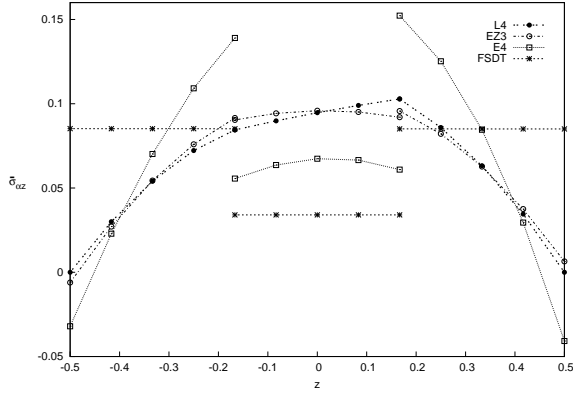


Figure 5: Shear stress $\bar{\sigma}_{\alpha z}$. $R/a = 5$ and Figure 6: Normal stress $\bar{\sigma}_{zz}$. $R/a = 5$ and $a/h = 100$. Symmetric lamination with $N_l = a/h = 100$. Symmetric lamination with $N_l = 3$.

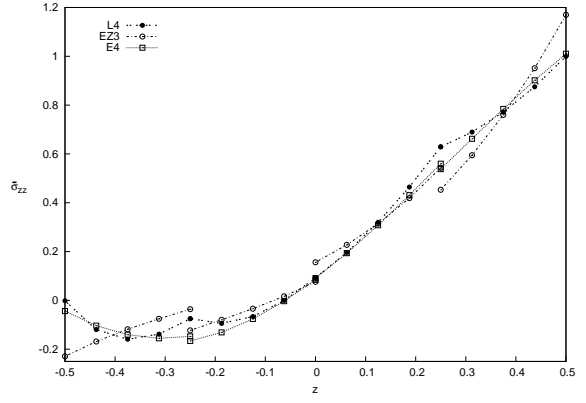
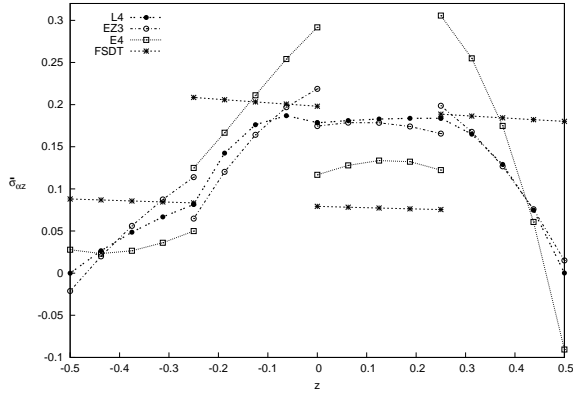


Figure 7: Shear stress $\bar{\sigma}_{\alpha z}$. $R/a = 1$ and Figure 8: Normal stress $\bar{\sigma}_{zz}$. $R/a = 1$ and $a/h = 5$. Anti-symmetric lamination with $a/h = 5$. Anti-symmetric lamination with $N_l = 4$.

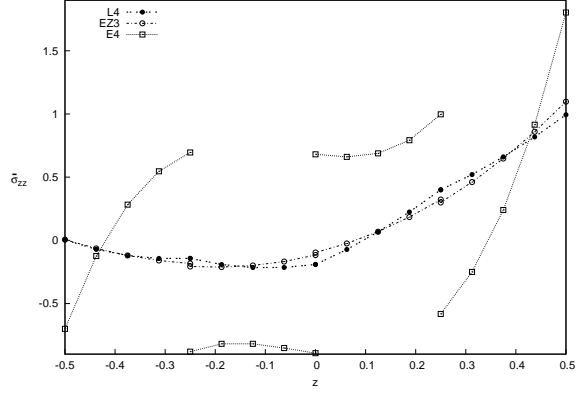
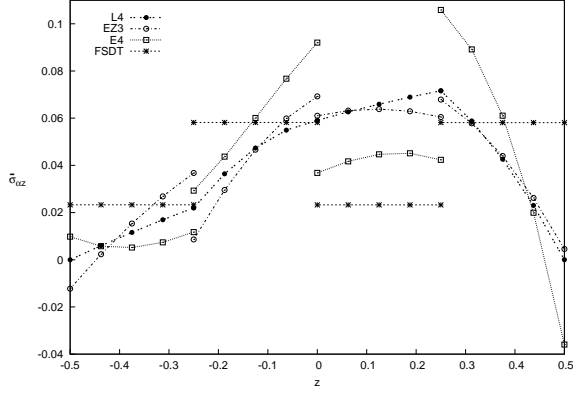


Figure 9: Shear stress $\bar{\sigma}_{\alpha z}$. $R/a = 5$ and Figure 10: Normal stress $\bar{\sigma}_{zz}$. $R/a = 5$ and $a/h = 100$. Anti-symmetric lamination with $a/h = 100$. Anti-symmetric lamination with $N_l = 4$.

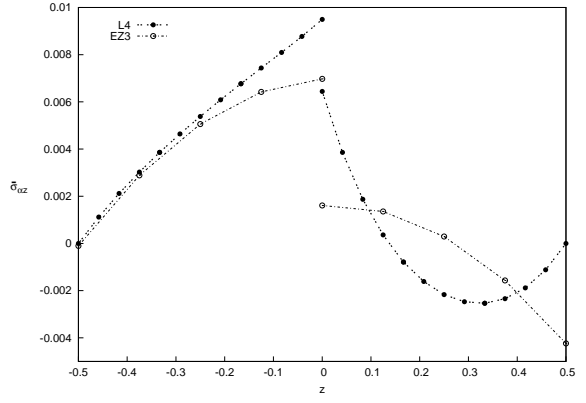
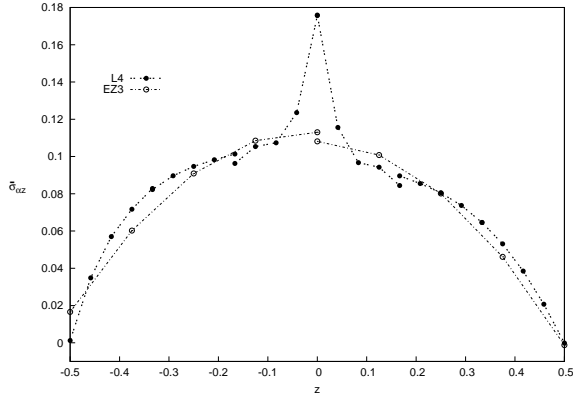


Figure 11: Shear stress $\bar{\sigma}_{\alpha z}$. $R/a = 1$ and $a/h = 5$. Lamination $(45^\circ, -45^\circ)$. Figure 12: Shear stress $\bar{\sigma}_{\alpha z}$. $R/a = 1$ and $a/h = 100$. Lamination $(45^\circ, -45^\circ)$.

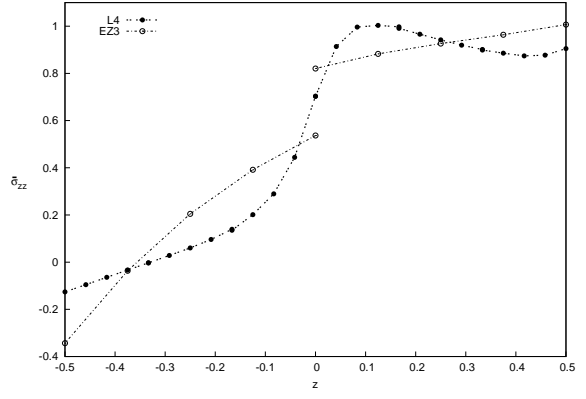
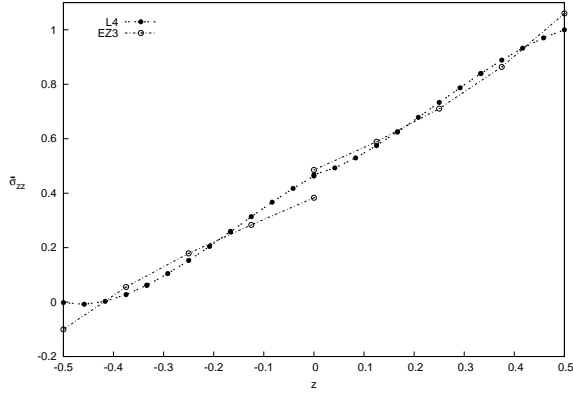


Figure 13: Normal stress $\bar{\sigma}_{zz}$. $R/a = 5$ and $a/h = 5$. Lamination $(45^\circ, -45^\circ)$. Figure 14: Normal stress $\bar{\sigma}_{zz}$. $R/a = 5$ and $a/h = 100$. Lamination $(45^\circ, -45^\circ)$.

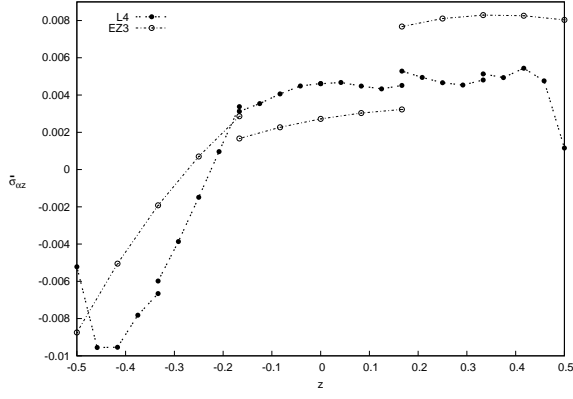


Figure 15: Shear stress $\bar{\sigma}_{\alpha z}$. $R/a = 1$ and $a/h = 5$. Clamped-free boundary conditions.

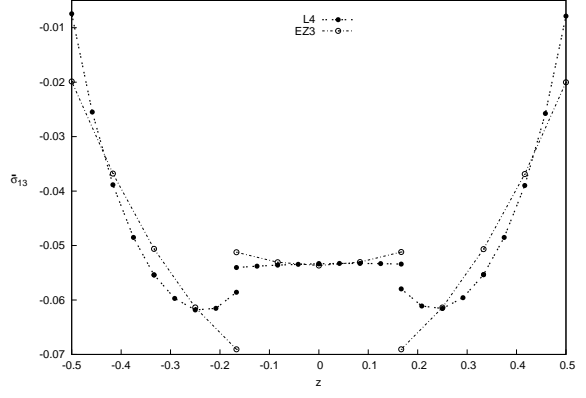


Figure 16: Shear stress $\bar{\sigma}_{\alpha z}$. $R/a = 1$ and $a/h = 100$. Clamped-free boundary conditions.

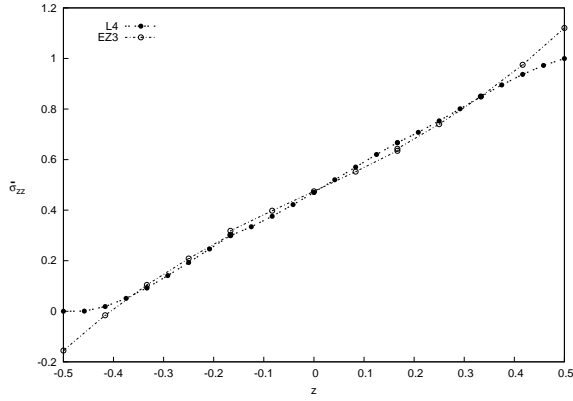


Figure 17: Normal stress $\bar{\sigma}_{zz}$. $R/a = 5$ and $a/h = 5$. Clamped-free boundary conditions.

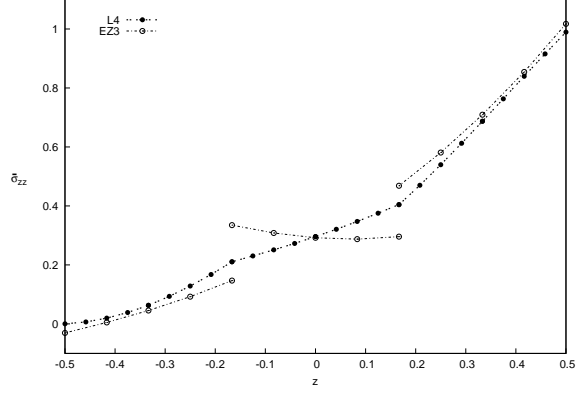


Figure 18: Normal stress $\bar{\sigma}_{zz}$. $R/a = 5$ and $a/h = 100$. Clamped-free boundary conditions.

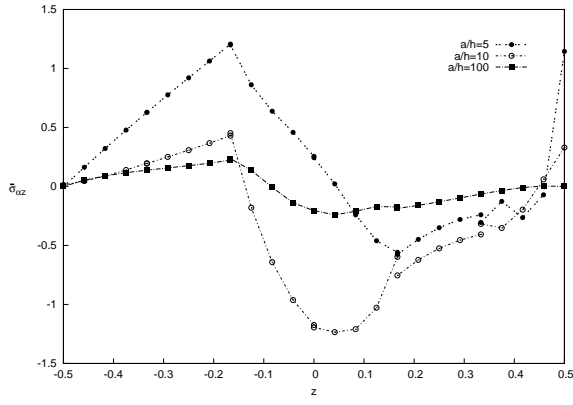


Figure 19: Shear stress $\bar{\sigma}_{\alpha z}$ by varying a/h for $R/a = 2$. Concentrated load.

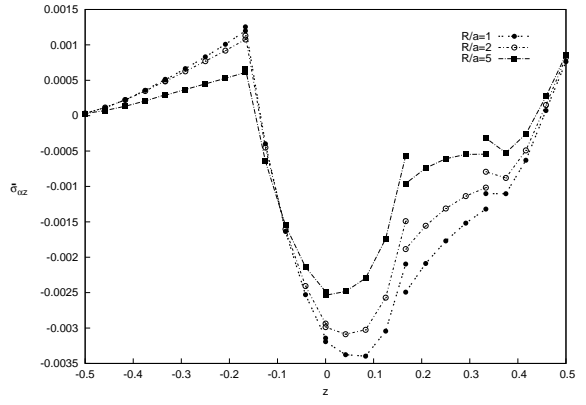


Figure 20: Shear stress $\bar{\sigma}_{\alpha z}$ by varying R/a for $a/h = 10$. Concentrated load.

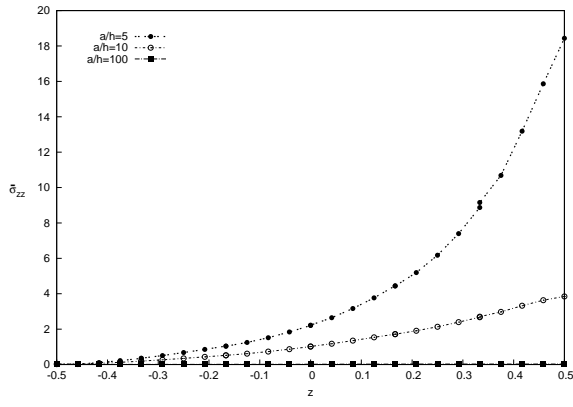


Figure 21: Normal stress $\bar{\sigma}_{zz}$ by varying a/h for $R/a = 2$. Concentrated load.

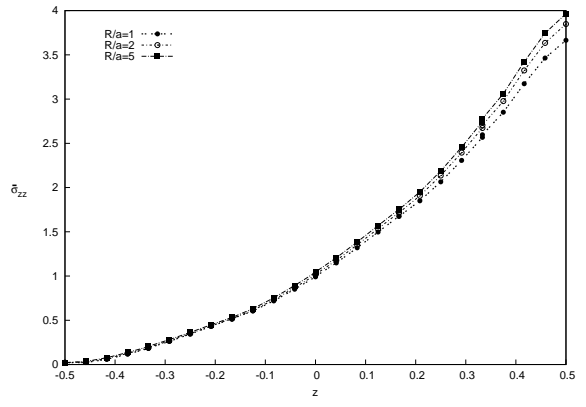


Figure 22: Normal stress $\bar{\sigma}_{zz}$ by varying R/a for $a/h = 10$. Concentrated load.